OXIDATIVE COUPLING OF METHANE OVER Mn/Na_2WO_4 CATALYST SUPPORTED BY MONOLITHIC SiO_2

by

Çağla Uzunoğlu

B.S., Chemical Engineering, Marmara University, 2014

Submitted to the Institute for Graduate Studies in
Science and Engineering in partial fulfillment of
the requirements for the degree of
Master of Science

Graduate Program in Chemical Engineering

Boğaziçi University

2016

to my family

ACKNOWLEDGEMENTS

At first, I would like to convey my gratitude to my thesis advisor, Prof. Ramazan Yıldırım. This work would not be possible without his acknowledgement and experiences. With his guidance and insistence, this work was accomplished. Besides that, he was always patient, kind and encouraging to me during the whole period of this work. He brings me different perspective during my research and keeps my interest and excitement on this project. Furthermore, I would like to thank my thesis co-advisor, Prof. Ahmet Kerim Avcı for his support. I would like to express my sincere gratitude to my thesis committee members; Prof. Ahmet Erhan Aksoylu, Assoc. Hasan Bedir and Assist. Prof. Mehmet Erdem Günay for sparing their valuable time. Their comments contributed a different perspective for my study.

Heartfelt thanks to Aybüke Leba for her friendship, motivation, and endless support. I always feel very lucky to have her. Her assistance and encouragement help me a lot during my experiments. Very special thanks to Melek Selcen Başar for her friendship, kindness and support during my thesis. I cannot imagine the period of the thesis preparation without her everlasting assistance.

I also want to express great appreciation for Manouchehr Nadjafi for his valuable helps and comments. I am very grateful to work with all CATREL team, especially, Aysun İpek Paksoy, Elif Can, Merve Eropak, Çağla Odabaşı, Ali Uzun, Burcu Acar, Dilara Saadetnejad, Cihat Öztepe, Merve Can, Sinan Koç, Amin Delpharish, Elif Erdinç and Serhat Erşahin.

I would like to thank to my friends in graduate class; İrem Ezgi Dayan, Hatice Eyvaz and Sevde Üçpınar for their friendliness and making this period enjoyable. Moreover, I want to thank my friends Buket Süslü, Zeynep Akçay, Ece Biberoğlu, Gamze Ayran and Murat Sükuti for their patience and motivation throughout my life. They make this process enjoyable and pleasant. Cordial thanks to Bilgi Dedeoğlu, Yakup Bal, Melike Gürbüz and Başak Ünen for their technical assistence during my thesis.

Finally, I would like to express my dearest gratitude to my beloved family; my father, Bayram Uzunoğlu, my mother, Ayşe Uzunoğlu and my brother, Uğur Çağatay Uzunoğlu for their patience, advice, everlasting encouragement and moral support throughout my entire life. The words are not enough to describe my gratefulness to my family. For this reason, this thesis is dedicated to them.

ABSTRACT

OXIDATIVE COUPLING OF METHANE OVER Mn/Na_2WO_4 CATALYST SUPPORTED BY MONOLITHIC SiO_2

In this study, oxidative coupling of methane (OCM) to ethane and ethylene was investigated over Mn/Na_2WO_4 catalyst supported by monolithic silica. Monolithic silica (monosil), which was prepared using sol-gel method, composed of white whole-structural rods with meso and macroporosities; 2 wt.% Mn and 5 wt.% Na_2WO_4 were impregnated respectively to the monolithic silica by dropping the precursor solution over the support by injection needle. OCM reaction was carried out by using a 10 mm ID quartz reactor. After the catalyst bed, inside diameter of the reactor was reduced to 2 mm in order to hinder the non-selective gas phase reactions. For comparison particulate catalyst prepared by incipient to wetness impregnation method and wash-coated catalyst over the commercial cordierite monolith was also tested. The results have shown that performance of monosil (about 16% C_2 yield) is comparable with particulate catalyst, which have given the best results (about 19% C_2 yield); the wash coated catalyst over the commercial cordierite monolith did not worked well (maximum yield was about 6%). Besides, the C_{2+} selectivity and yield over the monosil catalyst remained the same for a long time on stream indicating that the monosil catalyst is very stable for OCM reaction. It was also observed that monosil regained its activity, after increasing the temperature from and then decreasing to the optimum temperature (no hysteresis effect). Therefore, it was concluded that Mn/Na_2WO_4 catalyst over monosil can be a promising alternative for the OCM process.

ÖZET

MONOLİTİK $Mn/Na_2WO_4/SiO_2$ KATALİZÖRÜ ÜZERİNDE METANIN OKSİJEN VARLIĞINDA YÜKSEK HİDROKARBONLU MOLEKÜLLERE DÖNÜŞÜMÜ

Bu çalışmada, monolitik silika bazlı Mn/Na_2WO_4 katalizörü üzerinde metanın oksijen varlığında etan ve etilene dönüşümü (OCM) incelenmiştir. Sol-jel yöntemiyle üretilen monolitik silika (monosil), mezo ve makroporlardan oluşan beyaz, çubuk şeklinde bir yapıdır. %2 Mn ve %5 Na_2WO_4 verecek şekilde metal çözeltileri bir dereceli şırınga yardımıyla monosil yapıya emdirilmiştir. OCM reaksiyonu, 10 mm iç çapında kuvars bir cam reaktör ile gerçekleştirilmiş, reaktörün katalizör yatağından sonraki kısmının çapı 2 mm'ye düşürülerek oluşan ürünleri seçici olmayan ürünlere dönüşmesi engellenmiştir. Reaksiyon sonuçlarını karşılaştırmak için ıslak emdirme yöntemi ile elde edilen toz katalizör ve ticari cordierite monolit yüzeyine Mn/Na_2WO_4 yüklenmesi ile elde edilen katalizörler de test edilmiştir. Elde edilen sonuçlar, monolitik silika yapısındaki katalizörün performansının (C2 verimi yaklaşık %16) en iyi performansa sahip olan toz katalizör (C2 verimi yaklaşık %19) ile kıyaslanabilir olduğunu göstermiştir. Kordiyerit monolit üzerindeki performans ise düşük olmuştur (C2 verimi yaklaşık % 6). Bunun yanında, reaksiyon süresince monolitik silika yapılı katalizörün seçiciliğinin ve veriminin sabit kalması kararlı bir yapı olduğunun göstergesidir. Optimum sıcaklık testinden sonra yüksek sıcaklıklara çıkarılarak bir süre çalıştırılan katalizör tekrar optimum sıcaklığa soğutulduğunda ilk denemede gösterdiği performansı göstermiştir (histerik etki görülmemiştir). Böylece monosil bazlı Mn/Na_2WO_4 katalizörün OCM prosesi için umut vaat eden bir alternatif olabileceği sonucu çıkartılmıştır.

TABLE OF CONTENTS

LIST OF FIGURES

LIST OF TABLES

LIST OF ACRONYMS/ABBREVIATIONS

CTMABr	Cetyltrimethylammonium Bromide
GC	Gas Chromatography
GHSV	Gas Hourly Space Velocity
MFC	Mass Flow Controller
OCM	Oxidative Coupling of Methane
PEG	Polyethylene Glycol
PEO	Polyethylene Oxide
PVC	Polyvinyl Chloride
TCD	Thermal Conductivity Detector
TEOS	Tetraethylorthosilicate
TMOS	Tetramethylorthosilicate

1. INTRODUCTION

Methane is the primary component of the natural gas. The production of valuable hydrocarbons from methane necessitates reforming reaction, which demands an elevated pressure and temperature (Schuurman *et al*., 2015); the strong C-H bonds of methane make its utilization difficult. The absence of functional group, magnetic moment or polar distribution provides a stable nature for methane, which causes tremendous operation costs for utilization (Lunsford, 1995). For this reason, oxidative coupling of methane is considered a promising route for its conversion into C_{2+} hydrocarbons. OCM offers a direct route by circumventing the expensive syngas step (Lunsford, 2000). The most accepted mechanism of OCM consists of two different reaction processes as the heterogeneous catalytic and the non-catalyzed gas phase reactions. The desirable products come from the heterogeneous catalytic reactions whereas the gas phase reactions cause the formation of CO_x products (Alavi and Shahri, 2008).

Although OCM is considered the most suitable and easiest way to obtain C_{2+} products, many obstacles prevents the commercialization of this process. Especially, the temperature control in the catalyst bed complicates the heat treatment during the process (Alavi and Shahri, 2008). This problem has deceived the researchers about the temperature of the catalyst bed. Several studies have shown that this problem causes at least a 150 °C temperature difference between the catalytic zone and the reactor furnace (Pak and Lunsford, 1998; Cameron *et al.*, 1990).

Various catalysts have been investigated to overcome the obstacles of the OCM process and to enhance the C_2 selectivity and yield. However, ethane and ethylene yields have never exceeded 25% (Schuurman *et al.*, 2015). Among the alternatives tested, $Mn/Na_2WO_4/SiO_2$ has been found as one of the most effective catalyst for the oxidative coupling of methane. The $Mn/Na_2WO_4/SiO_2$ catalyst shows both high activity and stability during the OCM process (Palermo *et al*., 1998; Ji *et al.,* 2002; Baerns *et al.*, 2011). The interaction among Mn, Na and W metals provide the formation of the active centers on the surface of the support (Ji *et al.*, 2002; Wu *et al.,* 1995; Wang *et al.,* 1995). Each element in

the catalyst has a special role. Manganese acts as an oxygen supplier for active centers of tungsten due to its high electronic conductivity; the sodium has a dual role to produce desired products as well as to inhibit by-products and acts as a structural promoter (Palermo *et al.,* 1998, Ji *et al.,* 1999, Schuurman *et al*., 2015; Galadima and Muraza, 2016). Tungstate provides the formation of active sites both W=O and W-O-Si which compromise the active site for the OCM reaction. Thereby, the exchange between gaseous and lattice oxygen is enhanced considerably.

The composition of 2 wt.% of Mn and 5 wt.% of Na_2WO_4 give the most efficient results for the OCM reaction. Several researchers have also tested other compositions, but they indicated that increasing the percentage of the precursors causes decreasing the yield (Koirala *et al.,* 2014; Ji e*t al.*, 2002; Ji *et al.,* 1999). Therefore, the compositions of each element keep constant for the best results. Moreover, the positive effect that is provided by Mn, W and Na is diminished easily when any of these three elements is replaced with a something else. This indicates that only a combination of manganese, sodium and tungsten has a special role for the high performance of $Mn/Na_2WO_4/SiO_2$ catalyst (Somaley and Reza, 2011; Jiang *et al*., 1993).

The operation conditions of the OCM process are also important to achieve high selectivity and yield. Because of the nature of the methane, high temperature is compulsory. In various studies, it is observed that the temperature between 600-800 °C is needed for a successful OCM reaction (Tiemersma *et al.,* 2012). However, higher temperature also causes the catalyst deactivation; consequently, the formation of by-products becomes favorable (Korf *et al.,* 1989). Desirable yields strongly depend on the feed composition as well. Nevertheless, detection of the optimum feed composition is crucial because the gas phase reactions may easily dominate the process (Yagobi, 2011; Mleczko, 1995).

By considering that the some of the reactions are in the gas phase, some investigator argued that the void structure of the catalyst should play a role in OCM reactions. In this study, OCM process was investigated over monolithic forms (with various void structure), of the $Mn/Na_2WO_4/SiO_2$ to investigate this matter further. For this purpose, wash coated cordierite monolithic catalyst as well as the monolithic silica (monosil), which is prepared

using various methods were studied under the various feed compositions and the reaction temperature, and compared with the particulate catalyst.

Chapter 2 gathered the basic information about the oxidative coupling of methane process from the literatures until today. Firstly, the reaction mechanism was investigated in order to understand the conditions enhancing the ethylene yield. Detailed information was given about the reason of the CO_x formation to help the reduction of the by-products and increasing the desirable products. Then the chapter focused on the $Mn/Na_2WO_4/SiO_2$ catalyst by examining the role of each individual component. After the effects of the reaction, parameters were investigated, Chapter 2 concluded with the catalyst preparation methods. The experimental system and the steps of the catalyst preparation were explained in Chapter 3 in detail. In Chapter 4, the results of this study were presented and discussed while the conclusion of the experimental study and recommendation for the future work are summarized in Chapter 5.

2. LITERATURE SURVEY

2.1. Oxidative Coupling of Methane

Oxidative coupling of methane is a promising route to produce ethane and ethylene from the natural gas directly. However, OCM has not been commercialized due to the lack of complete understanding of the relation between catalyst properties and reaction conditions. Currently, many investigations have been working to find out a suitable catalyst and to reveal the reaction mechanism behind of OCM.

2.1.1. Limitations of Oxidative Coupling of Methane

Oxidative coupling of methane reaction has gained much attention since it was first reported by Keller and Bhasin in 1982. Obtaining hydrocarbons that are more useful such as ethylene and ethane directly from methane make OCM intriguing. However, this process has not been commercialized because the following factors:

(i) C_{2+} selectivity and yield are too low,
(ii) Technological novelty results is uncertainty for scale-up,
(iii) High separation costs for by products.

Heat management is also an important engineering problem for coupling of methane since it is an exothermic reaction and the excess heat causes the formations of carbon oxides not only reduces the selectivity, but also increase the heat of the reaction. The other crucial obstacle for converting methane directly to more valuable products by heterogeneous catalysts is the low selectivity at high conversion, which is due to the higher reactivity of the products than methane (Holmen, 2009). Developing an industrially reliable and stable OCM catalyst and carrying out the reaction at low temperatures are quite difficult (Galadima and Muraza, 2016).

Nowadays, researchers have been dealing with reaction engineering aspect and catalyst improvement in order make this process technically feasible and economical (Tiemersma *et al.*, 2012). A total yield higher than 35-40% provides an economically feasible system. Various aspects as reaction kinetics, reactor selection and different modes of reactor operation are analyzed with the aim of identifying reaction engineering in order to maximize C_{2+} selectivity and yield. Particularly, available kinetic models for reaction engineering applications are revised and the importance of various reaction steps, as well as pre- and post-catalytic reactions has been investigated. Since the OCM is a complex reaction network of parallel and consecutive, heterogeneous and homogeneous reaction steps, the selectivity to C_{2+} hydrocarbons strongly depends on the reaction conditions; reaction variables such as GHSV, temperature and CH_4/O_2 ratio play an important role on the catalytic performance of OCM (Karimi *et al.*, 2007). Following sections focus on the reaction mechanism and the effect of the reaction conditions over oxidative coupling of methane and examine the most promising catalyst, which is $Na_2WO_4/Mn/SiO_2$ catalyst.

2.1.2. Reaction Mechanism

The reaction mechanism of oxidative coupling of methane has not been understood fully since it includes complex network involving many heterogeneous and homogeneous gas phase reactions. Many kinetic models have been developed with varying complexity, depending on the surface and gas phase reactions. The OCM reaction mechanism can be divided into three parts as adsorption of oxygen species, catalytic surface reactions and gas-phase reactions containing 14 reaction steps, which were proposed by Lee *et al*. (2012) as shown in the Figure 2.1.

First two steps of Figure 2.1 are referred to the dissociative adsorption of oxygen molecules. Lee *et al.* (2012) proposed that methane adsorption occurred by Eley-Rideal type of reaction mechanism. After adsorption of the oxygen species, gaseous methane was assumed to combine with atomic oxygen on the catalytic surface. Rideal-type mechanism took place wherein methane molecules adsorb to produce methyl radicals on the oxidative surface and hydrocarbons form from desorbed gaseous radicals. Furthermore, ethylene is produced from ethane by the reactions R_2, R_3, R_{13}, and R_{14}. Production of ethylene is carried

out by the consecutive dehydrogenation of ethane and additional hydrogen abstraction of ethyl radical (C_2H_5•). However, side reactions, which include the formation of CO_x molecules, also take place not only on the catalytic surface but also in the gas phase, which is presented in Figure 2.1 by reactions R_4, R_5, and R_6. Moreover, CO can be formed when CH_3 and C_2H_3 radicals react with gaseous oxygen molecules.

Adsorption	A_1 : $O_2 + 2s \underset{k^{rev}_{O_2}}{\overset{k_{O_2}}{\rightleftharpoons}} 2O(s)$	$\left(K_{O_2} = k_{O_2}/k^{rev}_{O_2}\right)$
	A_2 : $2OH(s) \underset{k^{rev}_{H_2O}}{\overset{k_{H_2O}}{\rightleftharpoons}} H_2O + O(s) + s$	$\left(K_{H_2O} = k_{H_2O}/k^{rev}_{H_2O}\right)$
Catalytic surface reactions	R_1 : $CH_4 + O(s) \xrightarrow{k_1} CH_3\bullet + OH(s)$	
	R_2 : $C_2H_6 + O(s) \xrightarrow{k_2} C_2H_5\bullet + OH(s)$	
	R_3 : $C_2H_5\bullet + O(s) \xrightarrow{k_3} C_2H_4 + OH(s)$	
	R_4 : $CH_3\bullet + 3O(s) \xrightarrow{k_4} CHO(s) + 2OH(s)$	
	R_5 : $CHO(s) + O(s) \xrightarrow{k_5} CO + OH(s) + s$	
	R_6 : $CO + O(s) \xrightarrow{k_6} CO_2 + s$	
	R_7 : $C_2H_4 + O(s) \xrightarrow{k_7} C_2H_3\bullet + OH(s)$	
Gas-phase reactions	R_8 : $2CH_3\bullet \xrightarrow{k_8} C_2H_6$	
	R_9 : $CH_3\bullet + O_2 \xrightarrow{k_9} CHO\bullet + H_2O$	
	R_{10} : $C_2H_3\bullet + O_2 + OH\bullet \xrightarrow{k_{10}} 2CHO\bullet + H_2O$	
	R_{11} : $CHO\bullet + O_2 \xrightarrow{k_{11}} CO + HO_2\bullet$	
	R_{12} : $CO + HO_2\bullet \xrightarrow{k_{12}} CO_2 + OH\bullet$	
	R_{13} : $C_2H_6 \xrightarrow{k_{13}} C_2H_5\bullet + H\bullet$	
	R_{14} : $C_2H_5\bullet + H\bullet \xrightarrow{k_{14}} C_2H_4 + H_2$	

Figure 2.1. Reaction mechanism of oxidative coupling of methane for $Mn/Na_2WO_4/SiO_2$ catalyst (Lee *et al.*, 2012).

Furthermore, the first step (R_1) of the catalytic surface reactions, which is the hydrogen abstraction from methane shown in Figure 2.1, plays an important role for a proper OCM reaction mechanism. In this step, methane interacts with an active surface oxygen species. This interaction must result in the abstraction of a hydrogen atom (or a proton plus an electron). In other words, the surface oxide must be able to accommodate

the electron in addition to the proton, which forms the surface hydroxyl in order to achieve successful results. For this reason, it is crucial that the oxygen is attached to a redox active metal, which can accept the electron. Unreactive surface oxide is needed, so that methyl radical can escape from the catalyst surface and react with another gas-phase methyl radical to form ethane. The interaction between the methyl group and the surface determine the formation of the products. If the interaction is too strong, an adsorbed methoxy group can form which is then oxidized to CO and CO_2 by additional surface oxygen. The hydroxyl group that form during hydrogen abstraction will react or disproportionate to form water which desorbs and leaves an oxygen vacancy. To close the catalytic cycle, the oxygen vacancy is regenerated by gas-phase oxygen (Elkins *et al*., 2015).

Takanabe and Iglesia (2009) claimed that the most important step in the OCM i.e. hydrogen abstraction is more favorable when H_2O is available since it simplifies the formation of OH-included reactions. Nevertheless, when H_2O concentration exceeds a certain amount it influences the O_2 pressure and conversion along the reactor, so it makes the system complicated.

2.1.3. Ethane and Ethylene Formation from Methane Coupling

Two different methods for ethylene production have been currently commercialized. Those are naphtha steam cracking and ethane thermal cracking processes. However, these technologies have some difficulties. Firstly, heat treatment is necessary in order to crack the C-C and C-H bonds to convert naphtha or ethane into ethylene. Besides that, CO_2 emission is another crucial problem. Galadima and Muraza (2016) reported that three tons of CO_2 could be emitted for every single ton of ethylene produced. For these reasons, huge efforts have been spent to find a better and environmental friendly solution by researchers. Therefore, OCM has been considered a potential method to produce ethylene.

Tiemersma *et al.* (2012) proposed that during the methane coupling reaction, ethylene could be formed either by oxidative dehydrogenation or by thermal cracking of ethane as shown in Equations 2.1 and 2.2 respectively.

$$C_2H_6 + \frac{1}{2}O_2 \rightarrow C_2H_4 + H_2O \quad (2.1)$$

$$C_2H_6 \rightarrow C_2H_4 + H_2 \quad (2.2)$$

Chen *et al.* (1994) investigated co-feeding ethane with methane and oxygen to a reactor in the absence of a catalyst. They found that overall conversion enhanced greatly and this led to an increased radical concentration and hence higher branching rates. Nevertheless, when the ethane to methane inlet radio exceeded 0.04 this beneficial effect diminished.

Salehoun *et al.* (2008) suggested that C_2 formation enhances in the absence of gas-phase oxygen. In this way, Mn-Na_2WO_4/SiO_2 catalyst provides its lattice oxygen for the reaction. At higher temperature, the lattice oxygen usage for OCM was carried out effortless since oxygen can move easily. However, they observed that temperature higher than 800 °C causes decreasing of C_2 formation whereas increasing CO_x products, especially carbon monoxide. After this consequence, they concluded that selectivity of C_2 products increase with existence of the surface lattice oxygen whereas the bulk lattice oxygen leads to mainly to carbon oxide products particularly, CO formation.

2.1.4. Carbon Monoxide and Carbon Dioxide Formation as By-products

In the OCM reaction, CO_x's are considered as undesirable by-products, which have negative effect on the OCM reaction system. Ross *et al.* (1989) explored the influence of CO_2 on the OCM over the Li/MgO catalyst. They found that CO_2 in the gas phase lowered both the CH_4 conversion and the yield of C_2 products. In the other research of Shi *et al.* (2015), they investigated the effect of the co-feeding CO_2 on the OCM mechanism by using $Mn/Na_2WO_4/SiO_2$ catalyst. CO_2 in the feed gas caused the transformation of active Na_2WO_4 species into inactive $MnWO_4$ species, which caused dramatically, decrease in CH_4 conversion and C_2H_4 selectivity.

The gas phase radicals in the OCM reaction network may enter into chain reactions that result in the formation of CO and subsequently CO_2. Experiments that have been

carried out until today have demonstrated that at small conversion levels most of CO_2 is derived from CH_4, but at commercially significant conversion levels, C_2H_4 would be the dominant source of CO_2. Additional experiments have shown that this occurs mainly via heterogeneous reactions. One of the challenges in catalyst development is to modify a material so that the secondary reaction of C_2H_4 will be inhibited while the activation of CH_4 will still occur (Eppinger *et al*., 2014).

There exist several reaction pathways leading to CO_x formation. CO_2 is formed via methyl radical by the sequential hydrogen abstraction from methoxy species on the catalyst, via hydrogen abstraction from ethane and ethylene and heterogeneous oxidation of ethylene by an adsorption step (Alexiadis *et al.,* 2014). CO molecules occur on the catalytic surface easily due to the high reactive nature of ethylene. Moreover, CO_x formation reactions are thermodynamically favored as illustrated in Figure 2.2.

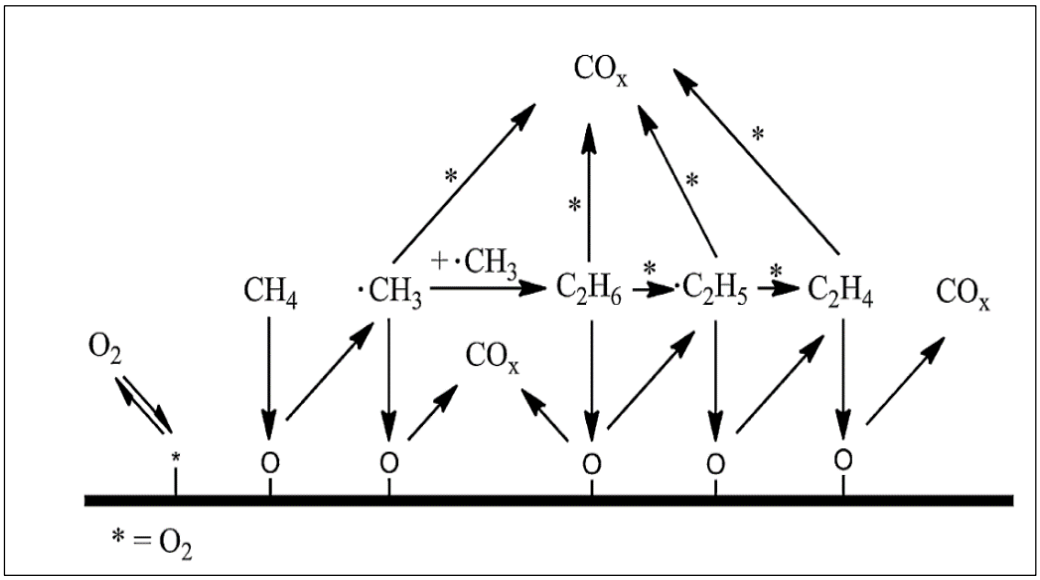

Figure 2.2. Formation of CO_x molecules during OCM reaction (Beck *et al*., 2014).

On the other hand, Shi *et al.* (2015) claimed that the presence of proper amount of CO_2 in the OCM reaction system leads to changes over $Na_2WO_4/Mn/SiO_2$ catalyst structure and improves the catalytic performance of $Na_2WO_4/Mn/SiO_2$ to ethylene formation since CO_2 promotes the migration of Na, W from the catalyst bulk to the surface. However, Al-Zahrani *et al.* (1994) proposed that CO_2 loading to the feed lowered the activity and C_2

yield with negligible effect on selectivity. This opposite results might be due to type of the catalyst since Shi *et al.* (2015) was used $Na_2WO_4/Mn/SiO_2$ catalyst whereas Al-Zahrani *et al.* (1994) worked with Li/MgO.

Koirala *et al.* (2014) proposed that CO formation increased promptly when CO_2 formation decreased simultaneously at high temperature. This was because of the reverse water gas shift shown in Equation (2.3) (Nikoo *et al*., 2011).

$$CO_2 + H_2 \rightarrow CO + H_2O \quad (2.3)$$

2.2. $Mn/Na_2WO_4/SiO_2$ Catalyst for Oxidative Coupling of Methane

Development of an effective catalyst for oxidative coupling of methane remains to be the most challenging and crucial step in the commercialization of this process. Until now, a variety of catalysts has been investigated for OCM reaction. Researchers have been focused on finding a suitable catalyst with highly active and providing convenient C_2 yield and selectivity. Beside those, impact on the down streaming unit operations and the thermal reaction characteristics of the reactor have been taken into account for obtaining a suitable OCM catalyst. Apart from those, catalyst properties such as basicity, specific surface area as well as effect of reaction conditions plays an important role for achieving optimal C_{2+} yield (Rane *et al*., 2008; Koirala *et al*., 2014). Baerns *et al.* (2011) examined papers that were published in the last 30 years and they concluded that multicomponent catalysts have shown typically better performance compared to pure metal oxide based catalysts.

Among the studied OCM catalysts so far, $Mn\text{-}Na_2WO_4/SiO_2$ is one of the most stable and recommended catalyst. The interactions between Na, W and Mn with the SiO_2 support create the active sites of the catalyst, while at the same time retaining its stability (Godini *et al*., 2014). Each metal has a different attribution in the way to a successful OCM process. These effects are discussed in the following parts.

2.2.1. The Role of Sodium over Oxidative Coupling of Methane

Ji *et al.* (2002) studied the effect of the Na, W and Mn amount over the oxidative coupling of methane. They observed that Na amount between 0.4-2.3 wt.% plays an important role to obtain high yield over the OCM reaction. The highest yield was obtained with an amount of 1.6 wt.% sodium. With increasing the Na amount causes a decrease over conversion and selectivity of ethylene and carbon dioxide whereas ethane and carbon monoxide formation increase dramatically. Thus, these results suggest that Na has an essential component to achieve high conversion and yield over OCM reaction. Moreover, it provides not only high C_2H_4 yield but also low CO formation.

In another article, Ji *et al*. (1999) only focused on the effect of the sodium over OCM reaction. The total percentage of Na_2WO_4 was kept constant as 5% which contained normally 0.78 Na and 4.22 W. Different catalysts were prepared with a changing Na amount between 0 and 7.80 to observe the impact of sodium on selectivity. Without sodium, no C_2H_4 was formed and selectivity of C_2H_4 was increased with increasing amount of Na. Moreover, they concluded that CO_x formation showed the highest selectivity without sodium, but after adding Na, this amount started to decrease. Those results they obtained show that sodium has an essential role to produce desired products as well as to inhibit by-products (Ji *et al.,* 1999).

Koirala *et al.* (2014) claimed that Na_2WO_4 had an effect on the C_2H_4/C_2H_6 ratio. In the absence of the Na, the ratio was 0.7. However, after loadings of Na, this ratio started to increase indicating that ethylene formation from ethane is low in the absence of sodium.

Palermo *et al.* (1998) found that Na has a dual role as both structural and chemical promoter. Firstly, it induces conversion of the amorphous silica support to catalytically inert α-cristobalite. Secondly, it assists to dispersion of W over the surface and creation of the active sites by WO_4. Moreover, Ji *et al.* (2002) proved that without Na, octahedral WO_6 formation took place, so this caused a lower catalytic activity and selectivity. Therefore, it is proved that the modification of WO_4 with Na were very crucial for the formation of active centers.

Catalyst performance in the OCM reaction can be improved with increasing the basicity of the catalyst without causing any damage on the structure. According to the Galadima and Muraza (2016) sodium has a crucial role to increase the surface basicity, in this way more active catalyst is obtained for the reaction system. Moreover, Koirala *et al.* (2014) proposed that the interaction between Na and metal oxide provides a better activity for the catalyst.

2.2.2. The Role of the Manganese over the Oxidative Coupling of Methane

Jiang *et al.* (1993) investigated the effect of the Mn/SiO_2 catalyst in compared to the $Mn/Na_2WO_4/SiO_2$ catalyst. They observed that manganese interacts with silica support, and Mn-O-Si compound is obtained. Thus, it was proved that manganese has a role over the activity of the $Mn/Na_2WO_4/SiO_2$ catalyst. According to the XRD pattern they obtained, Mn was highly dispersed on the silica indicating that a strong interaction between Mn and SiO_2. However, no phase transition over SiO_2 was observed in spite of the high temperature calcination. This result showed that Mn has no active role over the transition to α-cristobalite phase.

Rodemerck *et al*. (2000) indicated that, without Mn, Na_2WO_4/SiO_2 catalyst showed a low activity. However, they claimed that Mn had no significant effect over the C_{2+} selectivity. This was mostly determined by Na_2WO_4 loading.

Koirala *et al.* (2014) found that in the absence of Mn, <1% yield at 5% conversion was obtained. After they added 1.9 wt.% Mn, they observed 18.5% yield. Manganese loading more than 1.9% caused a decline in both conversion and yield. Thus, they concluded that Mn has a significant effect for obtaining high yield. This result showed that Na-O-Mn component might be the active site for the reaction, which was also claimed by Wang *et al.* (1995). On the other hand, further increase of Mn cause the decrease in C_2 yield and higher than 5 wt.% Mn loading leads to formation of $MnMn_6SiO_{12}$ which enhance the non-selective reaction pathways. However, the formation of Mn_2O_3 favors the selective reaction pathways. Furthermore, Mn loading also affects the formation of CO_x products. Koirala *et al.* (2014) observed that the CO/CO_2 molar ratios were reduced when Mn was

added to the 3% Na_2WO_4/SiO_2 catalyst. This result showed CO_2 formation is more favorable by Mn.

Ji *et al.* (2002) claimed that Mn has a crucial role to inhibit CO formation during the oxidative coupling of methane. They observed that without manganese, CO was formed, after adding 3 wt.% Mn, C_2H_4 selectivity and conversion keep constant although there was no CO formation.

2.2.3. The Role of the Tungstate over the Oxidative Coupling of Methane

Ji *et al.* (2003) investigated the effect of the different additives on WO_4 tetrahedra and the WO_6 octahedra. They concluded that WO_4 tetrahedra achieved a C_2 selectivity six fold higher than WO_6 octahedra. This attributed to the tungstate tetrahedra's suitable geometry and energy matching properties with CH_4. They argued that both WO_4 and WO_6 might be formed during the catalytic reaction. Because of the more complex geometry of the WO_6, the bonds of the WO_4 and CH_4 were much closer to each other as shown in Figure 2.3. Consequently, WO_6 octahedron has a higher energy leading to an unstable phase. Because of these facts, WO_4 interacting with CH_4 showed more stable and higher selectivity and conversion than WO_6. According to the FTIR results they obtained, the WO_4 tetrahedron was formed with SiO_2 a stable interaction whereas the WO_6 octahedron had an unstable impact on amorphous SiO_2. However, WO_6 formation may be inhibited in the presence of Na (Koirala *et al*., 2014).

Ji *et al.* (2002) investigated the effect of W loading. They deduced that in the absence of W, combustion reaction took place and mainly CO_2 was produced. However, addition of 0.4-1.6% W provided an increase of the C_2H_4 selectivity and thereby, CH_4 conversion improved dramatically. Nevertheless, after an optimum loading which is about 8.9% W, a decline was observed in both conversion and selectivity.

Palermo *et al.* (1998) claimed that tungstate might create surface bond structure as one W=O and three W-O-Si which compromise the active site for the OCM reaction. Thereby, the exchange between gaseous and lattice oxygen is enhanced considerably. On

the other hand, Ji *et al.* (2002) and Wu *et al.* (1995) proposed that Na-O-W and Na-O-Mn might be the other active centers due to distorted tetrahedral structure of WO_4.

Somaley and Reza (2011) prepared 4.5% M-9% Na-2.8% Mn/SiO_2 catalyst, in which M indicates the W, Cr, Nb and V. Thereby, they tested the influence of tungstate comparing with other active metals. Their results revealed that the highest C_{2+} selectivity and yield was obtained for W with the following order: W>Cr>Nb>V. However, no significant change on the conversion was detected.

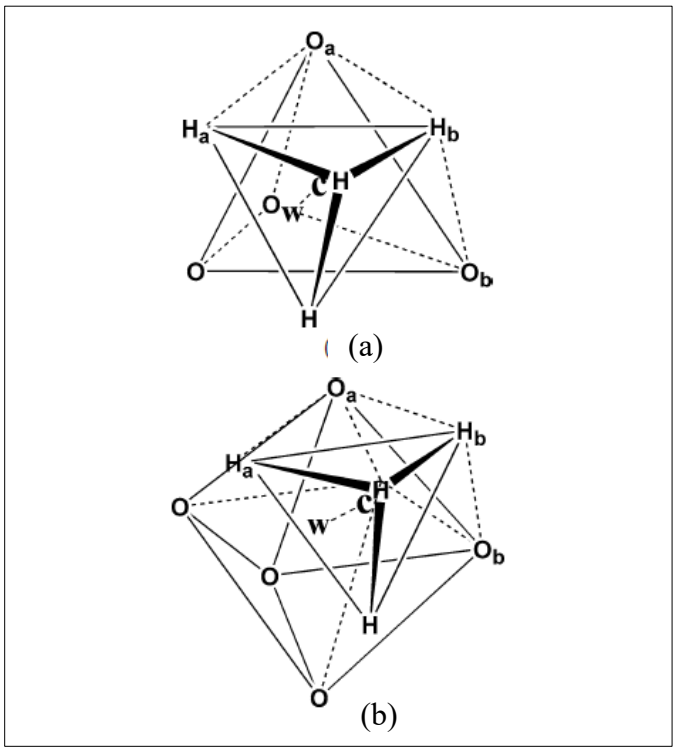

Figure 2.3. (a) Transition complex model of methane with WO_4 tetrahedron, (b) Transition complex model of methane with WO_6 octahedron (Ji *et al.,* 2002).

2.2.4. Silica as a Support for the Oxidative Coupling of Methane

Silica is used as the support material for Mn/Na_2WO_4 catalyst. Palermo *et al.* (1998) investigated that silica changes its form after catalyst impregnation. This transition of the amorphous silica to α-cristobalite provides active and highly selective catalyst in contrast

to active but unselective nature of the amorphous silica. This crystallization of α-cristobalite brings about a low surface area. In general, low surface area is undesirable for heterogeneous catalyst, but this is not valid for OCM, because low surface area inhibits the unwanted side reactions on the surface and provides an increase in C_2 selectivity (Elkins *et al*., 2015).

Palermo *et al.* (1998) made experiments in order to find the effect that caused the transition to α-cristobalite since this effect renders to create the transition at lower temperature than its normal temperature. By this way, it makes a huge impact on the C_2 selectivity and conversion. For these reasons, they prepared samples containing only Mn, W and Na other than the $Na_2WO_4/Mn/SiO_2$ catalyst. The results showed that in contrast to only Mn or W species, which had no effect on the transition to α-cristobalite, Na provides this transition to α-cristobalite. Therefore, it was concluded that Na has a dual role on the OCM reaction mechanism as both structural and chemical promoter. Although only W is not effective for the transition, it was observed that W loading enhanced the formation of highly crystalline α-cristobalite even at 750 °C. Additionally, very good selectivity towards ethylene was found.

Elkins *et al.* (2015) investigated the differences between SiO_2 and MgO as a support on the $Mn\text{-}Na_2WO_4$ by using XRD and XPS. They obtained from XRD results that the presence of Na_2WO_4, Mn_2O_3 and the α-cristobalite phase on the catalyst surface provides a high activity OCM catalyst. However, for the MgO supported catalyst no α-cristobalite and M_2O_3 was detected and Na_xWO_y compounds were formed on the surface. These results indicated that SiO_2 ensured stabilizing Na_2WO_4 compound. Besides that, Mn_2O_3 enhances the oxygen mobility between the gaseous and surface phases. This effect also ensured a high activity for the catalyst supported on silica. Moreover, according to the Pak and Lunsford (1998), MgO supported catalyst lost its activity dramatically with time on stream due to a drastic drop in methane conversion. Another reason is that MgO was inactive that Mn composed of an inert mixed oxide (Mg_6MnO_8) or appeared as Mn^{4+} in MnO_2. Therefore, MgO support was not able to stabilize Na_2WO_4 and Mn_2O_3 phase, which was achieved by SiO_2.

2.3. Effects of the Reaction Conditions

An active and stable catalyst is needed in order to increase C_2 products and reduce the CO_x formation. However, obtaining an effective catalyst is not enough to reach the target; the best set of reaction conditions should be also selected. For this reason, several studies have been continued to find out the optimal conditions to achieve desired results for oxidative coupling of methane. By changing the reaction conditions such as reactor parameters, CH_4/O_2 ratio, temperature, space velocity and pressure, methane conversion and C_2 yield can be improved. The conditions that have impacts on the heterogeneous and homogeneous reaction steps of the oxidative coupling of methane are elucidated in the following sections.

2.3.1. Influence of the Reactor Parameters

The design of the reactor has crucial effects on the oxidative coupling of methane. One of the reactor features that may be important is its shape. Düşova (2014) suggested that a reactor with a reduced diameter is favorable to increase C_2 selectivity. Lee *et al.* (2012) was also used this type of reactor by narrowing the reactor section of the post-catalytic region. However, they observed that a reduced diameter might cause the pressure drop. For this reason, they investigated the appropriate value for this part of the reactor. When the inner diameter of the reactor was below 3 mm, pressure drop could exist. Therefore, 4 mm was chosen. For the wider part of the reactor, 7 mm and 10 mm were tested. Since 7 mm part caused about a 0.7% pressure drop, 10 mm was preferred for the this part of the reactor. Additionally, Koirala *et al.* (2014) used 2 mm reduced diameter after the catalyst bed in order to reduce to dead volume.

Another crucial properties of the reactor is the position of the catalyst bed. Lee *et al.* (2012) proposed that catalyst must be located above the lower part of the central chamber in order to protect the desirable products from homogenous gas phase reactions. In other words, this modification inhibits the CO_x formation from the C_2 products.

The reactor filling material also influences the route of the OCM reaction. When the empty space of the reactor is filled with an inert material, methane conversion and ethylene selectivity increase significantly. The most important reason of this effect seems that such materials are able to delay the heating of reaction gases to the high temperatures before the catalyst bed. By this way, a big portion of the homogeneous side reactions can be minimized (Lee *et al.,* 2012). Different type of filling material was tested by several researches. Koirala *et al.* (2014) filled the empty space of the reactor with SiC and quartz wool. They observed a negligible change on the conversion (1-2%). Lee *et al.* (2012) tested various filling material. They packed the reactor with inert ZrO_2-SiO_2 beads to inhibit the high temperature gradient between the empty space of the reactor and the catalyst bed. However, some homogeneous side reactions took place under the inert ZrO_2-SiO_2. Besides that, quartz chips were tested as packing materials, but changes on the conversion and C_2 selectivity were almost same in the case of the quartz chips or ceramic beads. Nevertheless, they preferred to use ceramic beads due to their well-shaped instead of non-uniform shaped of quartz chips.

2.3.2. The Effect of the Feed Gas Composition

Methane to oxygen ratio influences the OCM reaction deeply. More oxygen feed provide more formation of ethylene. However, the amount of oxygen affects the carbon oxides production mostly. For this reason, the oxygen concentration in the feed is normally taken lower than methane concentration to prevent CO_x formation even though oxygen seems to also increase of methane conversion.

Yagobi (2011) investigated the changes of yield and conversion with varying methane to oxygen ratio and GHSV (gas hourly space velocity). He tested suitability of the $Sn/BaTiO_3$ catalyst under the 1, 2, 3, 4 and 7.5 CH_4/O_2 ratio and 8000-12000 h^{-1} GHSV. He concluded that in all situations, there is a decline of methane consumption with decreasing GHSV. The decrease of the methane conversion was because of the lower contact time, so C_2 hydrocarbons were favorable. After he tested all ratios above, he concluded that the optimum methane to oxygen ratio was 2. However, increasing the O_2 concentration caused an enhancement of the combustion reaction, which was undesired. As

a result, selectivity also reduced. In spite of these disadvantageous, CH_4/O_2 ratio of two was desirable because oxygen is the initiator of the OCM reaction i.e. assists to reach the required activation energy of methane decomposition. Additionally, with the help oxygen the formation of methyl radicals is getting easier leading to higher C_2 production.

Tiemersma *et al.* (2012) indicated that oxygen concentration in the feed is one of the most important parameter to achieve a successful OCM reaction. The reason for this is that oxygen acts as a surface species. In order to sustain the OCM reaction, a continuous oxygen supply is needed on the catalyst surface. Additionally, Sofranko *et al.* (1987) claimed that molecular oxygen was necessary for a high methane conversion (15-20%) with a high C_2 selectivity (80-90%).

Mleczko *et al.* (1995) proposed that the higher C_{2+} selectivity is achieved when CH_4/O_2 ratio is considerably low. On the other hand, high methane conversion is obtain when oxygen amount in the feed is increased, this have also positive impact on the C_{2+} yield. This contradiction is the biggest impediment to make the OCM commercially available.

2.3.3. The Effect of the Temperature

In order to achieve high C_2 yield and methane conversion, the influence of the temperature is incontrovertible. Although OCM is an exothermic reaction in total, a significant heat is needed to break the C-H bonds in methane. C_{2+} selectivity and conversion are enhanced with increasing temperature. However, if the reactor temperature keeps going to rise, non-selective gas phase reactions become dominant; thus, C_{2+} yield starts to decline. For this reason, an optimum temperature is necessary for the oxidative coupling methane reaction (Tiemersma *et al.,* 2012).

A crucial problem reported by several researchers is the hot spot formation in the catalyst bed. Since the thermocouples are located outside wall of the reactor, there is a consensus that the real temperature in the catalyst bed is much higher than the temperature displays in the thermocouple. Pak and Lunsford (1998) investigated the hot spot formation

over the $Mn/Na_2WO_4/SiO_2$ and $Mn/Na_2WO_4/MgO$ catalysts. A 150 °C temperature difference was observed between catalyst bed and the reactor furnace. In another study carried out by Cameron and his co-workers indicating the hot spot of 150 °C over La_2O_3 catalyst. Moreover, more than 200 °C temperature differences were obtained during OCM reaction with a La_2O_3/CaO catalyst. These results pointed out that the high magnitude of the temperature profiles (hot spots) exist due to the high activation energy of the methane. However, this is not the only reason for hot spot formation. Both methane to oxygen ratio and the catalyst activity play an important role for this effect (Pak and Lunsford, 1998; Cameron *et al*., 1990).

High temperature causes also faster catalyst deactivation. Korf *et al.* (1989) indicated that Li/MgO catalyst endure for 100 h operation. Although a 20% C_2 yield was obtained above 825 °C, the quick deactivation of the catalyst interrupted the process easily. Thus, the limitation of the reactor temperature can be changed this negative effect on the reaction conditions. On the other hand, the more stable nature of $Mn/Na_2WO_4/SiO_2$ makes this catalyst more resistive to much higher temperature than Li/MgO. Thereby, a wider temperature range for the $Mn/Na_2WO_4/SiO_2$ is available (Tiemersma *et al.,* 2012).

2.3.4. The Effect of the Pressure

The total pressure of the reaction influences the all process including the C_2 yield and undesirable products formation. Mleczko and Baerns (1995) reported that at elevated pressure, C_2 selectivity decreased gradually over Li/MgO, Sm_2O_3 and Sr/ Sm_2O_3 catalysts, but when empty reactor was tested, there was no influence on the C_2 selectivity. Therefore, it was concluded that at moderate pressures an optimum selectivity could be obtained. The similar results were obtained for the PbO/Al_2O_3 catalyst. The same selectivity was obtained at pressures between 01-0.4 MPa. However, at least 70 °C higher temperature was needed at 0.4 MPa pressure in order to reach the same result.

At high pressures apart from the selectivity, the conversion of CO to CO_2 decreases significantly. If the increases of the pressure keeps going above 1000 kPa, gas phase reactions take place both pre and post catalytic region (Tiemersma *et al.,* 2012).

$Na_2WO_4/Mn/SiO_2$ catalyst was also tested over a wide range of total pressure from 100 to 800 kPa. It was observed that the pressure higher than 600 kPa caused increasing by-products. Additionally, many studies were carried out under atmospheric pressure and high selectivity and conversion was obtained (Ji *et al.,* 2012; Tiemersma *et al.,* 2012).

Ekstrom and co-workers conducted an experiment over Li/MgO in order to observe the effect of the temperature. Changing the pressure from 0.1 to 0.5 MPa only altered the CO/CO_2 ratio in the product stream. Consequently, a threefold increase in conversion was observed because of the gas phase reactions.

2.3. Reactor Selection for Oxidative Coupling of Methane

Due to the high exothermic nature of the OCM various types of reactor has been proposed like fixed beds, fluidized beds, membrane reactors, reactors with molten salts, reverse-flow reactors and countercurrent moving-bed reactors. However, until now researchers preferred mostly fixed beds and fluidized beds. Still modifications on these reactors have been carried and new reactor designs have been tested in order to increase the activity and the selectivity of the OCM reaction (Mleczko *et al.*, 1994). For these reasons, the following sections focus on not only the packed bed reactors as one of the conventional reactor type but also a novel design such as monolithic silica (monosil) reactor.

2.3.1. Packed Bed Reactors

The most common reactor type in the process of the oxidative coupling of methane is the packed bed reactors. This type of reactors provide safer process operation, better control reaction parameters and easier product recovery (Sachse *et al.,* 2012). However, heat management, broad distribution of residence time and temperature control is the key challenge for the applications of this reactor for OCM processes. Therefore, Baerns and Hinsen (1986) proposed staged feeding of oxygen to the reactor. They observed that this method provided a uniform heat released and improved C_{2+} selectivity. Moreover, in the study of Mleczko and Baerns (1994) a modified fixed bed reactor was used which had a reduced diameter of 3 mm after the catalytic section. With this modification, the influence

of gas phase reactions reduced. The same results was obtained by Düşova (2014) who compared the activity of the reduced diameter reactor and a fixed inlet diameter reactor. She indicated that the reduction in the diameter increase the selectivity of the desirable products. Godini *et al.* (2014) claimed that, apart from the alteration over the reactor shape, higher methane to oxygen ratio could overcome the heat due to the reaction.

2.3.2. Monolithic Silica (Monosil) Structured Reactors

Monolithic silica can be defined as materials, which consist of silica constituents with multimodal macro-/mesoporosity (Sachse *et al.,* 2012). When monolithic structured catalysts are inserted into the conventional packed-bed reactors they bring several advantages along like reducing the pressure drop, overcoming heat and mass transfers limitations, preventing mechanical attrition and increasing the contacting efficiency. However, chemical deactivation of the catalyst has remained an unsolved problem even for monolithic reactors. Still, narrow size distribution, high specific surface area and large pore volume bring a breakthrough in the realm of the ordered mesoporous materials (Babin *et al.,* 2007; Smatt *et al.,* 2003). In their study of Sachse and coworkers (2011), they proposed that the geometric shape of monolithic body can overcome the drawbacks of the continuous packed-bed processes such as hot-spot formation and the formation of stagnation zones.

This type of reactor is very suitable for gas phase reactions or catalytic combustions (Mason *et al.,* 2007). High thermal and mechanical stability as well as easy generation of a variety of catalytic active sites at the surface must be taken into account in order to use such reactions. When the mesoporous monoliths inserted into catalytic reactors this allows an efficient and rapid mass transport through the material with a minimal operation pressure and mass to volume ratio. The structure of monolithic catalyst consists of parallel channels or foams with interconnected mesopores, which supply a fast diffusion to and from the active sites (Sachse *et al.,* 2007; Ahmed-Omer *et al.,* 2006).

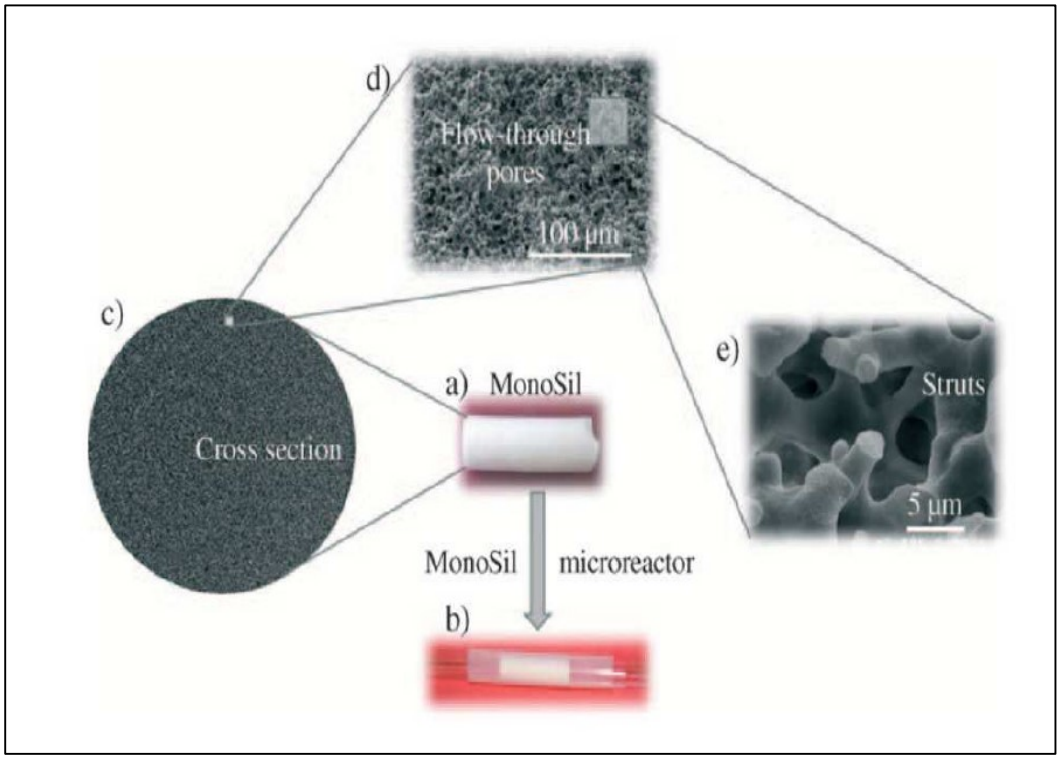

Figure 2.4. Monolithic silica structured representation; (a) monosil after preparation, (b) monosil in the microreactor, (c) SEM images, (d) flow through pores, and (e) struts (Kadib *et al.,* 2009).

Monolithic support based on polymers was preferred as surface structure directing agent to form the fine mesopores. However, the swelling of these materials cause pressure drops limited thermal stability and mechanical resistance (Watt and Wiles, 2006). Fortunately, a complex with inorganic silica supports overcome these problems and is formed functionalized ordered mesoporous silica. This monolithic silica, which was obtained, by Sachse and co-workers (2009) exhibits a high mechanical strength. Additionally, these monolithic structures which is called as monosils provides a uniform radial distribution of voids and struts, a very narrow size distribution of pores as shown in Figure 2.4. With these feature, a flat flow profile and the same residence time for all reactants can be obtained (Sachse *et al.,* 2009).

Sachse *et al.* (2009) compared the efficiency of the batch, packed-bed and monosil reactor. They concluded that monosil showed the best features among them since it

provided a larger contact area between the reaction medium and the catalyst, a much shorter diffusion path for the molecules through the struts and inhibiting the accumulation of co-product on active sites.

2.4. Catalyst Preparation Methods

There are several methods for preparing $Na_2WO_4/Mn/SiO_2$ catalyst in the literature. In this section, the most common methods, i.e. impregnation, sol-gel and monolithic catalyst preparations are discussed.

2.4.1. Incipient to Wetness Impregnation Method

Incipient to wetness impregnation method is the conventional method to prepare supported catalyst. In this method, the metal precursor solutions are added to the support drop by drop under the vacuum so that the pores of the support can easily fill with the metal precursors. Thereby, an effective catalyst can be obtained which includes considerably fewer process steps. The active components, which are Na, Mn and W, can be well-dispersed over the support surface after impregnation. This enables a higher activity and selectivity during the OCM reaction.

Different catalyst preparation methods (incipient to wetness, slurry mixing and wet impregnation) for $Na_2WO_4/Mn/SiO_2$ catalyst for OCM was prepared by Li *et al.* (2006). The results show that incipient to wetness impregnation methods shows the highest catalytic activity for the OCM reaction since Na, Mn and W are mainly dispersed on the surface of the support. Since the amounts of the active components are significantly low, it must be paid great attention during the impregnation in order to prevent from any material loss (Lee *et al.,* 2012).

The active metals were impregnated on the silica support one by one in order to prevent from any precipitation and the chemical deterioration. After Mn solution was added to the support, the prepared slurry is kept at oven for 5-6 over at 130 °C. Then, the second

active metal impregnation is carried out with the same method, which was applied for the first active metal (Godini *et al.,* 2014; Malekzadeh *et al.,* 2002; Li *et al.,* 2006).

2.4.2. Sol-gel Catalyst Preparation Method

The sol-gel process can be considered a very promising method for preparing Mn-Na_2WO_4/SiO_2 catalyst. This process involves transformation of a sol to a gel. A sol can be defined as a colloid of small particles that are dispersed into a liquid. A gel is a rigid non-fluid mass and is usually a substance made up of a continuous network including a continuous liquid phase. Therefore, sol-gel reactions involve hydrolysis and condensation reactions of inorganic alkoxide monomers in order to develop colloidal particles (sol) and consequently convert them into a network (gel). A metal or metalloid element bound to various reactive ligands represents the precursor used to synthesize the colloids. Metal alkoxides are the reagents mostly used for this purpose due to their ease of hydrolysis in the presence of water. Alkoxysilanes, like tetramethoxysilane (TMOS) or tetraethoxysilane (TEOS), are extensively used for production of silica gels (Alothman, 2012).

In the sol-gel method, the process divides into five groups as listed below;

(i) hydrolysis of precursors-sol formation,
(ii) polycondensation of hydrolyzed precursors-gelation,
(iii) aging,
(iv) drying,
(v) calcination (Gawel *et al.,* 2010).

The most difficult part of preparing monolithic silica by sol-gel method is the drying step which is indicated above. During the silica formation, a series of reactions become as shown in Equations (2.4), (2.5) and (2.6).

$$\equiv\text{Si-OR} + H_2O \xrightarrow{hydrolysis} \equiv Si - O - H + ROH \quad (2.4)$$

$$\equiv\text{Si-OR} + \text{HO-Si}\equiv \xrightarrow{condensation} \equiv Si - O - Si \equiv \ + ROH \quad (2.5)$$

$$\equiv\text{Si-OH} + \text{HO-Si}\equiv \xrightarrow{condensation} \equiv Si - O - Si \equiv \ + H_2O \qquad (2.6)$$

The reversibility of the Equations (2.5) and (2.6) causes the destruction of the gel matrix due to reactions of alcoholysis and hydrolysis of the Si-O-Si bonds and etherification of the Si-OH bond. Nevertheless, two different solutions have been proposed for this problem. The first one is the optimization of hydrolysis of tetraalkoxysilane and polycondensation of the products by varying the acidity of the medium in the course of the sol-gel process with simultaneous removal of the alcohol in the form of highly volatile compounds. The second one is the addition of a drying control chemical additive (DCCA) which provides an increase in the size of pores. This allows a more uniform growth of the three-dimensional network of the gel matrix and to an increase in the degree of its reinforcement (Khimich, 2003).

In the aging step, washing in siloxane solution increases the stiffness and strength of the aerogel since the solution allows adding new monomers to the silica network. As a result, this process causes a decrease of the permeability of the prepared gel (Siouffi, 2003).

After these steps a double pore silica gel (macrospores and mesopores) monoliths can be obtained by using sol-gel reactions with phase separation and a subsequent solvent exchange treatment (Alothman, 2012).

Until now, three different monolithic silica preparation methods have been proposed (Nakanishi and Soga, 1992; Kirsching *et al.,* 2005; Babin *et al.,* 2007). One of these methods consist of the nanocasting process combined with large-structure-directing agents such as polymeric colloids, starch gels or gas foams in order to be used as macroporogenes during sol-gel process (Babin *et al.,* 2007). In the study of Nakanishi and Soga (1992), the sol-gel process contained both phase separation and gelation in an acidic media, which achieved during a hydrolytic sol-gel synthesis of silicon alkoxide precursors. Finally, using triblock-copolymer surfactants as water-soluble polymers utilized a single step hierarchical macro- and mesoporous monolithic silica process. However, in this method, one must focus on the exact amounts of the material since any small change in the composition may cause small macrospores formation due to the phase separation process.

Silica monoliths obtained by Babin and his team (2007) was white rods, which were exposed to volume shrinkage about 1 or 2 mm after drying. Macrospore sizes were measured as 2-20 μm by SEM. They observed that the solution became turbid after 2 h at 40 °C, then started to transform into gel from the bottom. Above of the solid part, ethanol from TEOS accumulated. The homogeneity of the prepared solution starts to diminish during the polymerization of the silica. This polymerization entails the repulsion force between the solvent and the silica phase. This step has crucial effect for obtaining a strong macro-/mesoporous silica rods. Different parameters influence the phase separation and the macropore size such as the amount of water, the amount of silica alkoxide, and the amount of polymer, the number of ethylene oxide groups per silica, the polymer weight and the temperature of the synthesis. They claimed that the treatment of ammonia solution enables to stabilize the silica rods and induces of a disordered mesoporosity since the size of the disordered mesoporosity is controlled by the temperature of the treatment and the basicity of the solution. By this way, more strong silica skeleton can be obtained. Julita and Jarzebski (2008) achieved the same observation. They observed silica monoliths have ultra large mesopores after the hydrothermal treatment in aqueous ammonia solution.

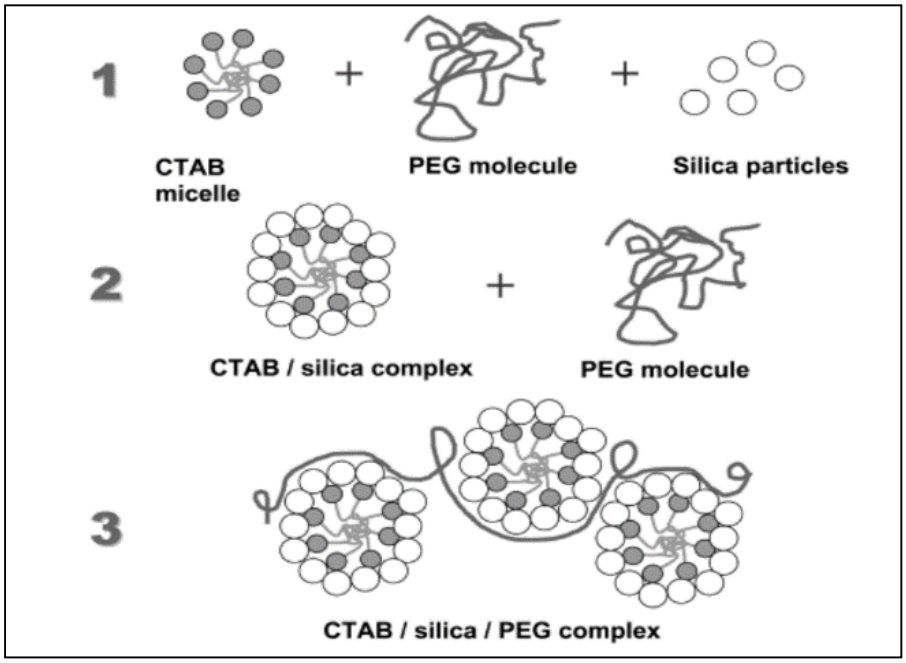

Figure 2.5. Monolithic silica preparation route with using a surfactant (CTAB) and a hydrogen-bonding homopolymer (PEG) as templates (Smatt *et al.,* 2003).

Babin and co-workers (2007) prepared another type of monolithic silica as MCM-41 monoliths with adding CTAB to transform the unstructured mesoporosity of the monolith skeleton into an ordered structured mesoporosity of MCM-41 type by pseudomorphic transformation. This means the architectures of the silica skeleton and of macroporosity remain while the mesoporous network transforms into more ordered one. The size of the macropores is dependent on the amount of CTAB in the solution. In other words, MCM-41 type monolithic silica provides not only an independent control of the macroporosity but also an ordered mesoporosity. The formation of such monolithic silica and the interaction of the CTAB, PEG and silica particles are visualized in Figure 2.5.

In addition to the CTAB, Siouffi (2003) proposed glycerol loading during sol-gel preparation enables narrow and uniform pore size distribution. Glycerol acted as a drying additive during the process, since it prevents further reaction of water.

Since monolithic silica provides both macro- and mesoporosities, an adequate diffusion of molecules through the catalyst pores allows the direct interaction with the acidic sites on the wall surface, which promotes a higher conversion. Additionally, the macropore structure inside the silica allows a fast mass transfer to the surface of the primary particles because the active sites of a supported catalyst are mainly located inside the primary particles (Giraldo *et al.,* 2007).

The monolithic silica structure can be prepared from a mixture including polymer, distilled water, alkoxysilane and catalyst to obtain a well-defined interconnected macroporous morphology. The gelation strongly depends on the duration of phase separation, the solubility of the constituents and the polymerization rate of silica. To speed up the gelation process, nitric acid can be used as a catalyst for hydrolysis. Polymer addition accelerates the gelation process (Nakanishi and Soga, 1992). Additionally, the use of polymers can simplify the control of the particle sizes due to its long hydrocarbon chain structure. For the monolithic silica preparation, the most common used polymer types are polyethylene glycol (PEG) and polyvinyl pyrrolidone (PVP) as the structure directing agent (Thirugnanam, 2013). Moreover, Martin *et al.* (2001) investigated the effect of PEG amount over silica structure. They observed that when the amount of PEG increased, the

mechanical stability and acoustic velocity decreases and vice versa. They also claimed that PEG addition can change pore size, clarity and surface area per gram.

According to the Smatt *et al.,* (2003), water-soluble polymers such as poly-ethylene oxide (PEO) provides to control the phase separation/gelation kinetics in the preparation of monolithic silica containing both interconnected macropores and textural mesoporosity. They claimed that macropore diameter could easily be controlled by adjusting the polymer concentration, since the timing of the phase separation relative to the sol-gel transition determines the macropore size. On the other hand, aggregation silica nanoparticles at the wall of the macroporous structure leads to formation of mesoporosity and the size of mesopores are dependent on the treatment of ammonia solution.

In another study of Sachse and his co-workers (2012), millimetric parallel multichannel reactors and macroporous silica monoliths was compared. It was indicated that macroporous silica monoliths showed better performance since it provides a higher surface to volume ratio and a very efficient mixing of fluids or reactants as a result of its interconnected nature of the macroporous network and lower macropore size at the micrometer scale.

Instead of SiO_2 supported Mn-Na_2WO_4 catalyst, Li and his coworkers (2008) tested Mn-Na_2WO_4/SiC for preparing monolithic foam catalyst and compared with SiO_2 based. They observed that specific properties of monolithic silica such as large exchange area, low-pressure drop and easy control of external porosity still remained after changing the support. Addition of those properties, hot-spot formation that always occurs over SiO_2 supported catalyst was not seen over SiC supported monolithic catalyst. This is because SiC is a refractory material which shows a high thermal conductivity.

Different templates have been proposed to prepare monolithic silica such as monoliths with foam-like macropores, worm-like macro-pores and interconnected sphere-like macropores. These different types can be formed by using polyurethane foams, phase-separated polymer liquids, colloidal crystals and surfactant micelle templates (Nishihara *et al.,* 2006; Witoon and Chaereonpanich, 2012; Shi *et al.,* 2003; Lenin *et al.,* 2005). For

example, Alvarez and Fuertes (2007) prepared a macro/mesoporous silica and carbon monoliths by using commercial polyurethane foam as template. They indicated that only mesopores limits the accessibility of the reactants to the inner part of the monolith. Therefore, a monolith with including macro/mesopores is more convenient. With the help of the polyurethane foam, they obtained a fully interconnected macroporous network with a well-ordered porosity.

2.4.3. Monolithic Catalyst Preparation Method

The term "monolith" is a combination of the two Greek words as mono means "single" and lithos means "stone". In general, monolith is referred to as the large uniform block of a single building material. In the realm of the heterogeneous catalysis, monoliths can be used as the support materials for the active metals. The most common monoliths used in industries and research laboratories are made of ceramic, which is known as cordierite monoliths (Tomasic and Jovic, 2006).

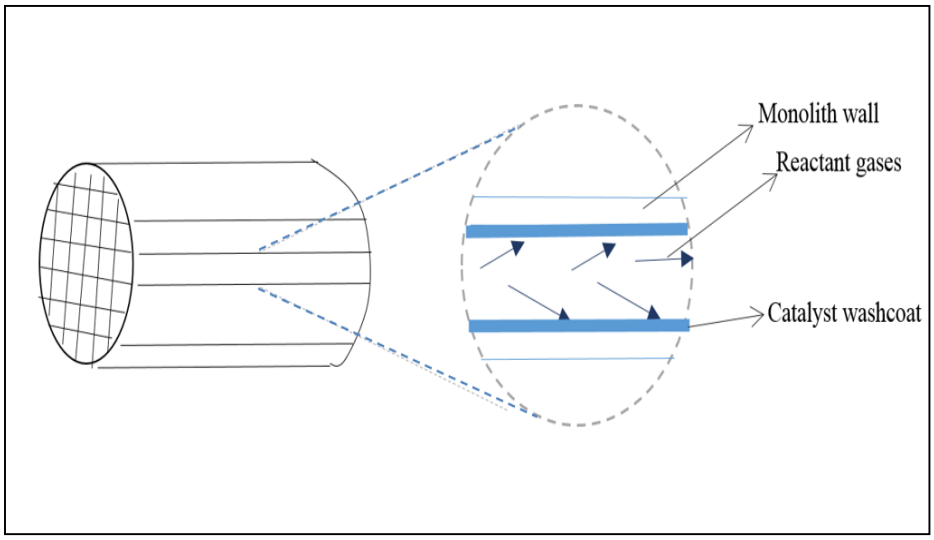

Figure 2.6. Schematic representation of the monolithic channel, when reactant gases passing through the catalyst surface.

In order to keep the precursors on the monolith walls, an appropriate support material is coated on the surface of the monolith before the impregnation of the precursors. These

support material is chosen based on the need of the type of precursor and the reaction mechanism. The most common supports that are used for coating monoliths are γ-Al_2O_3, SiO_2, ZrO_2, carbon and zeolites. These materials are coated through the channels of the monoliths in order to keep the precursors uniformly on the wall of the channels. During the reaction, reactant gases pass through each channel and interact with the catalyst on the walls and results products, which continue down the channel and exit (Farrauto *et al.,* 2001). The schematic representation of this procedure is shown in Figure 2.6.

Monolithic catalyst provides several advantages over conventional particle catalysts. These benefits can be arranged as high specific surface area, small pressure drop, good transfer by interphase diffusion through a catalytic layer, good thermal and mechanical properties and simple scale up (Moulijn *et al.,* 2001). The high specific surface area comes from the plurality of the channels, their diameter and wall thickness which indicates a large open frontal area. This allow to reduce the residence to flow and provides a low pressure drop, as a consequent lower energy loss (Farrouto *et al.,* 2001).

The most common ceramic catalyst used in the area of heterogeneous catalysis is the cordierite monolith, which have been commercially available since mid-1970s. These cordierite monoliths consist of extruded multi-cell channel with a chemical formula $2MgO.2Al_2O_3.5SiO_2$. The most significant characteristic of these monoliths is to ensure a low thermal expansion and high resistance to fracture due to the thermal shock with compared to other type of monoliths. Besides that, porosity and pore size distribution simplify the wash coat application and can act as a good wash coat adherence. Since cordierite monoliths have a melting point exceeds 1450 °C, a sufficient refractoriness can be assured for high temperature needed reactions (Williams, 2001).

Apart from these advantages, there are crucial disadvantages of the monolithic catalyst, especially for catalytic processes. The parallel channel monolith is essentially an adiabatic reactor limiting the control of the temperature since for many catalytic exothermic and endothermic reactions; selecting temperature has severe effect on the selectivity. For this reason, a metal monolith can be chosen, but for chemically controlled reactions, this

monolith may not contain sufficient catalyst to yield the desired conversion efficiencies (Farrauto *et al.,* 2001; Machado *et al.,* 2005).

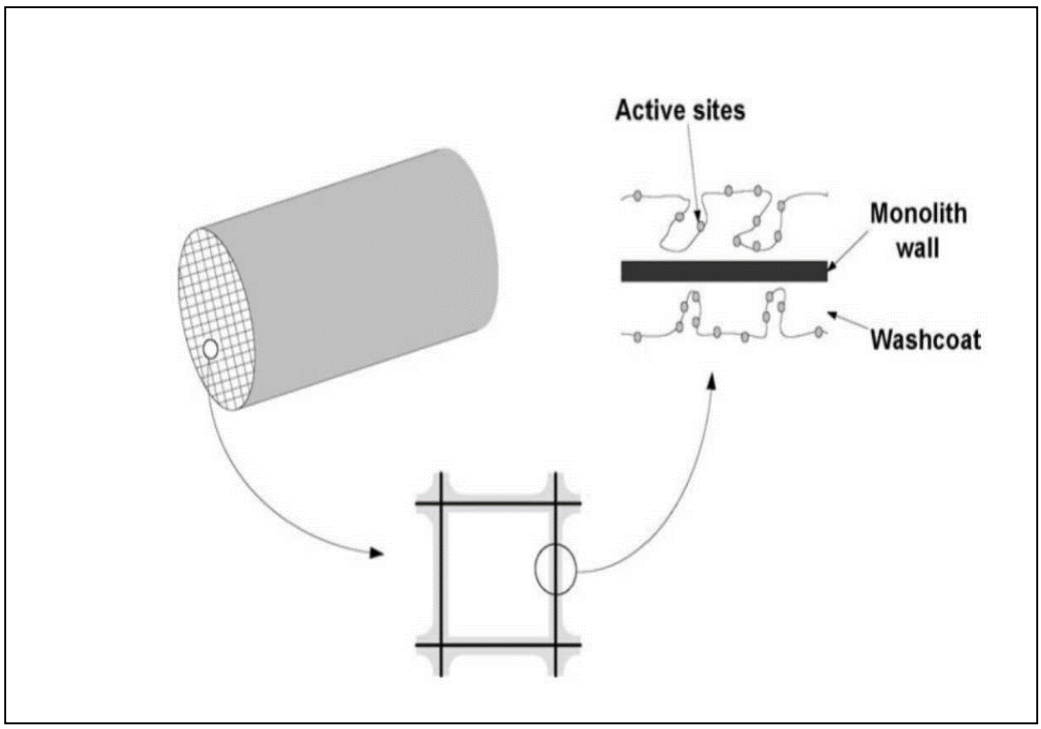

Figure 2.7. Schematic representation of monolithic catalyst and the location of the active sites (Tomasic and Jovic, 2006; William, 2005).

During the monolithic catalyst preparation, the most crucial part is that the active phase must be deposited on the inside walls of the inert monolith to enhance the surface area. The first step for the preparation is the coating of support material by wash-coating method. Thereby, the active sites can be placed on the surface of the supported material as shown in Figure 2.7.

The coating of the support can be accomplished by using several methods such as sol-gel method (the support in the liquid phase) or colloidal coating method (the support is in the form of suspended particles). In the colloidal coating method, the colloidal solution of silica or alumina is commercially available. In this procedure, monoliths are left in the colloidal solution for a particular time in order to ensure filling the channel with the solution and then excessive amounts are removed by blowing through air. Finally, they are dried in

the microwave. After obtaining high surface area supported monoliths, active precursors must be impregnated inside the channel walls by using wash coating or impregnation methods. The resulting monolithic catalyst is dried in an oven and calcined before testing under the OCM reaction (Tomasic and Jovic, 2006; William, 2005).

3. EXPERIMENTAL WORK

This chapter is divided into two parts as catalyst preparation and catalytic reaction system. After obtaining in their desired form, the catalysts were tested under the system that in in the Catalysis and Reaction Engineering Laboratory of Chemical Engineering Department, Boğaziçi University.

3.1. Materials

3.1.1. Chemicals

All chemicals that were used during the catalyst preparation in this study are shown in Table 3.1.

Table 3.1. Materials used during the experiments in the study.

Chemicals	**Formula**	**Purity**	**Source**	**Specification**	**Molecular Weight (g/mol)**
Acetic acid	CH_3COOH	≥99%	Merck	Aqueous solution	60.1
Ammonia solution	NH_3	≥99%	Aksın	25%	17
Colloidal silica	SiO_2	≥99%	Sigma-Aldrich	40 wt.% aqueous suspension	60.1

Table 3.1. Materials used during the experiments in the study (cont.).

Chemicals	**Formula**	**Purity**	**Source**	**Specification**	**Molecular Weight (g/mol)**
N-Cetyl-N, N, N-trimethyla-monium bromide (C_{16}TAB)	$C_{16}H_{33}N(CH_3)_3Br$	≥99%	Merck	Fine powder	364.5
Nitric acid	HNO_3	≥98%	Sigma-Aldrich	Aqueous solution	63.0
Polyethylene glycol 20,000	$HO(C_2H_4O)_nH$	≥98%	Merck	Aqueous solution	20000
Quartz Wool	SiO_2	≥99%	Leco	Fibrous	60.1
Sodium tungstate di-hydrate	$Na_2WO_4.2H_2O$	≥99%	Sigma-Aldrich	Fine powder	329.9
Tetraethyl orthosilicate (TEOS)	$C_8H_20O_4Si$	≥98%	Merck	Aqueous solution	208.3

3.1.2. Gases

Gases used in the experimental and feed analysis are listed in Table 3.2.

Table 3.2. Detailed explanation of the gases used in the study.

Gas	Formula	Specification	Type	Application
Carbon Dioxide	CO_2	99.995%	Product	GC Calibration
Carbon Monoxide	CO	99.5%	Product	GC Calibration
Ethane	C_2H_6	5% C_2H_6 balanced with He	Product	GC Calibration
Ethylene	C_2H_4	5% C_2H_4 balanced with He	Product	GC Calibration
Helium	He	99.998%	Inert	GC Carrier Gas, Reactor Cooling Gas
Methane	CH_4	99.995%	Reactant	GC Calibration
Nitrogen	N_2	99.998%	Standard	Gas Volume Change indicator
Oxygen	O_2	99.999%	Reactant	GC Calibration
Standard Mixture	CH_4-C_2H_6-C_2H_4	5%CH_4-2%C_2H_6-2% C_2H_4 balanced with He	Product	GC Calibration

3.2.1. Catalyst Preparation Techniques

In this part, different catalyst preparation techniques that were used during this study is listed below with the exhaustive explanations.

3.2.1.1. Particulate Catalyst Preparation with Impregnation Method. $Mn/Na_2WO_4/SiO_2$ particulate catalyst containing 2 wt.% Mn and 5 wt.% Na_2WO_4 supported on 60-100 mesh

size of pure SiO_2 were prepared by impregnation to incipient wetness of silica gel using the system in Figure 3.1. The aqueous solution of $Mn(NO_3)_2$ tetrahydrate and aqueous solutions of Na_2WO_4 dihydrate was impregnated on the pure silica separately.

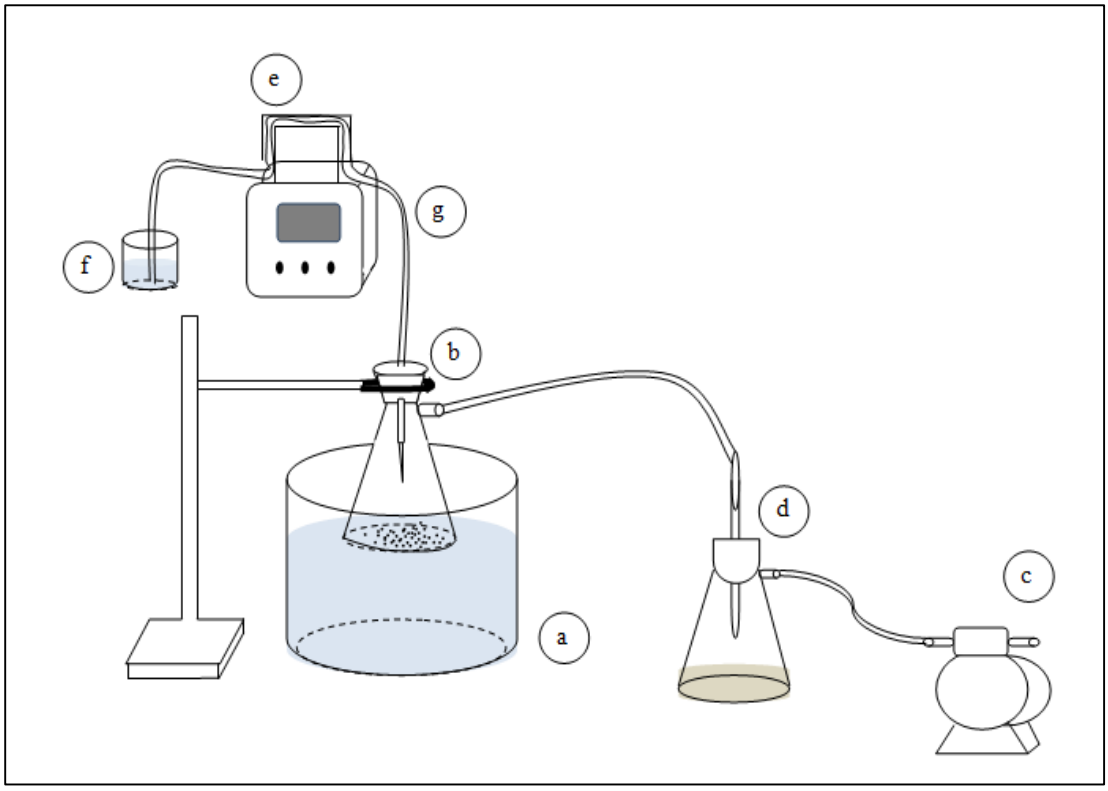

Figure 3.1. Schematic diagram of the impregnation system;
(a) ultrasonic mixer, (b) Buchner flask, (c) vacuum pump, (d) controller,
(e) peristaltic pump, (f) reactant storage tank, and (g) silicone tubing.

The system in Figure 3.1 consists of a Retsch UR1 ultrasonic mixer, a Buchner flask, a vacuum pump and a MasterFlex computerized-drive peristaltic pump. Solution started to pump from the reactant storage tank by the peristaltic pump. By passing through the silicone tubing, finally reached to the Buchner flask and impregnated over the support drop by drop under vacuum system. In order to prevent contamination in the vacuum pump, a controller was located between the system and the vacuum pump.

For the particulate catalyst preparation, a definite amount of 60-100 silica gel was weighed and mixed under a vacuum system for 30 minutes. Mn $(NO_3)_2$ tetrahydrate was

dissolved in deionized water on the basis 1 g silica gel/1.1 ml solution at 85 °C and the solution was fed to the vacuum flask at a flow rate of 0.5 $ml.min^{-1}$ by a silicone tubing using with a Masterflex computerized-drive peristaltic pump. After all solution was fed, it was ultrasonically mixed under vacuum for 30 min to obtain uniform distribution of the aqueous solution. The resulting slurry was separated from the vacuum system and dried at 130 °C for 5 h. The dried slurry was kept in the desiccator until cooling to 25 °C. Then, the slurry was used as the new support material and mixed under vacuum with ultrasonic mixer for 30 min. The appropriate amount of Na_2WO_4 with deionized water on the basis 1 g silica gel/1.2 ml solution was prepared with using the same procedure as before and fed to the vacuum flask. When all solution was fed, the slurry ultrasonically mixed until the all solution was homogeneously dissolved in the Büchner flask. Later, Mn/Na_2WO_4 impregnated silica was dried overnight at 130 °C and calcined at 800 °C for 8 h to obtained particulate $Mn/Na_2WO_4/SiO_2$ catalyst. Figure 3.2 shows the alteration of the particulate catalyst during impregnation process.

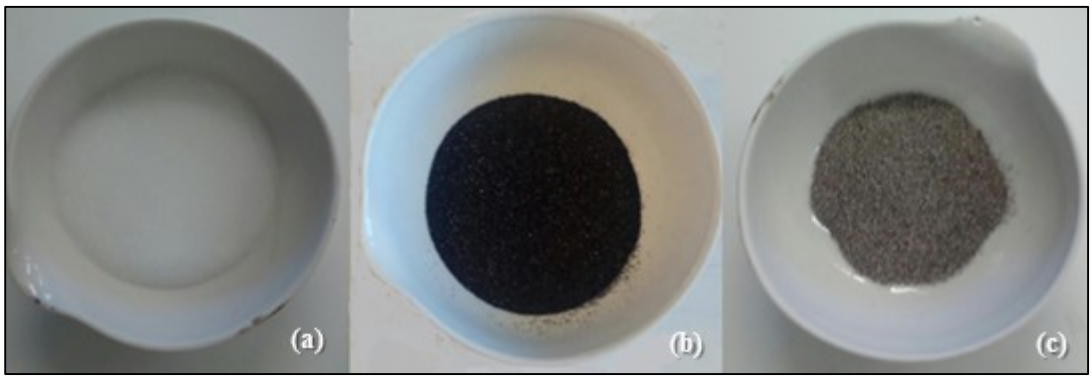

Figure 3.2. The formation of particulate $Mn/Na_2WO_4/SiO_2$ catalyst; (a) 60-100 mesh size silica gel, (b) particulate $Mn/Na_2WO_4/SiO_2$ catalyst after drying at 130 °C, (c) particulate $Mn/Na_2WO_4/SiO_2$ catalyst after calcination at 800 °C.

3.2.2.2. Monolithic Catalyst Preparation with Sol-gel Method. A programmable BS-302 type water bath was set at 0 °C and kept that temperature during the experiment. Since reaching the 0 °C takes about 1 h, it may be appropriate to operate the device before the experiment starts. For the solution circulation, a mixer adjusted in the water bath cabinet, so the homogeneity of the solution temperature is provided during the experiment. The

solution in the water bath was prepared based on the description in the manual of the device. According to the manual, antifreeze must be added for the 50% of the water bath and the remaining part was filled with the distilled water. Thereby, 8 L volume of the water bath filled with the antifreeze-distilled water solution to reach the desired temperature without damaging the device because the operation only with distilled water at 0 °C temperature may cause freezing at the bottom of the water bath. Thereby, serious disruptions may occur in the device.

For the preparation of sol-gel, 46.3 ml distilled water and 3.2 ml 69% nitric acid solution were mixed for 15 minutes at 0 °C. After that, 4 g PEG 20000 added to the beaker and was stirred for 1 h. Finally, 40.4 ml TEOS introduced and stirred 1 h until a gel was formed. In order to stabilize the temperature at 0 °C and avoid any rapid change of temperature, distilled water, nitric acid and TEOS kept in the freezer before adding to the solution. The physical properties of nitric acid and TEOS allow this conditions since freezing point of nitric acid is -42 °C and freezing point of TEOS is -82 °C.

After experiment finished, gel formation poured into different types of molds. An important parameter for the mold was its diameter; it cannot be larger than the reactor diameter since monolithic silica is easily broken after any force attempts. Nevertheless, a mold, which is larger 1 mm or 2 mm, is preferable because of the volume shrinkage during drying process. Glass tubes and syringes were used as the mold. However, the gel formation in the glass tubes created a non-uniform structure. Therefore, the different size plastic syringes were preferred as molds.

The solution in the molds was kept in the 40 °C oven for 5 days in order to complete the gelation and to separate from their molds easily. The gelation can be observed after 6 hours holding in the oven. To ease the evaporation on the solution, the length of the molds was shortened. Thereby, a homogeneous gelation of the monolithic structure was obtained.

After 5 days passed, monoliths were removed from their molds and were washed with deionized water, then treated 0.01 M ammonia solution for 20 h at 40 °C. Later, the obtained monolithic silicas were dried for 2 days at 40 °C. Finally, they were calcined for 5 h at

550 °C with a ramp rate of 1 °C/min. In this step, the most important point is the heating mechanism. When the monolith silica is put in the muffle furnace, which is at 550 °C, cracking is observed on the whole monolithic body. This causes the deformation of the monosils, which is not desired. Therefore, monosils were inserted into the muffle furnace at room temperature and then, heating of the furnace was started with an increase of 1 °C per minute until reaching 550 °C. Finally, monosils were kept 5 h at that temperature before leaving the cooling in the desiccator.

After calcination, each monolith was weighed in order to calculate the necessary amount of metal precursors. A definite amount of $Mn(NO_3)_2$ tetrahydrate solution was prepared for each monolith according to the same procedure which was explained in Section 3.2.1.1 and was applied with the help of a syringe or a disposable plastic transfer pipette. $Mn(NO_3)_2$ tetrahydrate impregnated monosils were then dried in the oven for 5 h at 130 °C. After monosils reached the room temperature in the desiccator, Na_2WO_4 dihydrate solution was applied to the monosils using with the same procedure. The monosils obtained were dried at 130 °C overnight, and then calcined at 800 °C for 8 h.

Another method to prepare monolithic silica with sol-gel method is the adding $Mn(NO_3)_2$ tetrahydrate solution during the gel formation. $Mn(NO_3)_2$ solution was introduced as a last component after TEOS. The final solution was stirred 20 more minutes and then poured into the molds. In this process, Na_2WO_4 solution could not be added to the solution because Na ions were collapsed at the bottom of the beaker since Na dissolve neither in Mn nor in the nitric acid solution.

After the solution was kept for 5 days in the oven and removing from the impurities with ammonia solution, Na_2WO_4 dihydrate solution was impregnated and then monosils were dried at 130 °C with a ramp rate of 1 °C/min for 5 h. For this procedure, initial calcination step at 550 °C was skipped since all precursors adding the system during the process was continued. The necessary amount of $Mn(NO_3)_2$ and Na_2WO_4 was calculated using data obtained from the previous sol-gel preparation. In the previous sol-gel preparation method, after the calcination step at 550 °C, the total weight of monosils was calculated. Based on this weight, the amount of $Mn(NO_3)_2$ and Na_2WO_4 can be calculated

for the second method since the same amount of ingredients was used. Since $Mn(NO_3)_2$ tetrahydrate solution was added during the sol-gel preparation, only one impregnation was carried out for Na_2WO_4. After drying at 130 °C in the oven, monosils were calcined. The calcinations step was performed in two different ways. The first one was calcination in the reactor by passing a definite percent of N_2 and O_2 gases. The second calcination procedure was the same as before which was at 800 °C in the muffle furnace.

Another method to obtain monolithic body, which was performed in this study, was MCM-41 silica monoliths. In this method, 26.5 ml deionized water and 1.2 ml nitric acid was mixed for 15 min. Then, 0.6 g of PEG 20000 was added and stirred for 1 h. Later, 22.2 ml TEOS was introduced to the system and continued to mix for 1 h. A final component, 8.8 g of N-Cetyl-N, N, N-trimethylammonium Bromide (C_{16}TAB) was added and stirred 30 min at 0 °C. The next steps were the same with the first method.

In Figure 3.3 demonstrates the three different types of monosils, which were prepared by using different methods. This pictures were taken after drying at 40 °C for 5 days when monosils were removed from their molds. Moreover, Figure 3.4 summarizes the all monolithic silica preparation process.

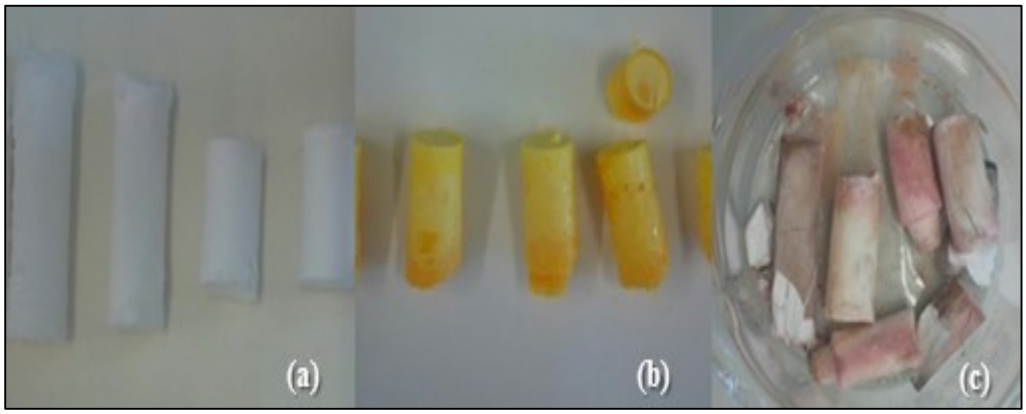

Figure 3.3. (a) Monolithic silicas after drying at 40 °C, (b) MCM-41 silica monoliths including C_{16}TAB, (c) monolithic silicas with Mn.

Figure 3.4. (a) Sol-gel preparation, (b) gel formation, (c) sol-gel in the molds, (d) in the oven, (e) after drying for 5 days, (f) monosils, (g) in ammonia solution, (h) dried monosils, (i) Mn impregnation, (j) Mn coated, (k) Na impregnation, (l) after calcination.

3.2.2.3. Preparation of Monolithic Support with Wash-coating. The commercial ceramic ($2MgO.2Al_2O_3.5SiO_2$) cordierite was used as monolithic support. Cordierite was first cut into dimensions 17 mm x 8 mm x 9 mm. 6 channels was obtained for each edge of the square and channels on the edges was removed so that it fits in the reactor easily. This cutting procedure of the cordierite monolith illustrated in Figure 3.5. Later, monoliths were washed with acetone to clean any impurities during the cutting procedure and then, dried in the oven for 1 h. After monoliths reached the room temperature in the desiccator, they were weighed to obtain the bare weights.

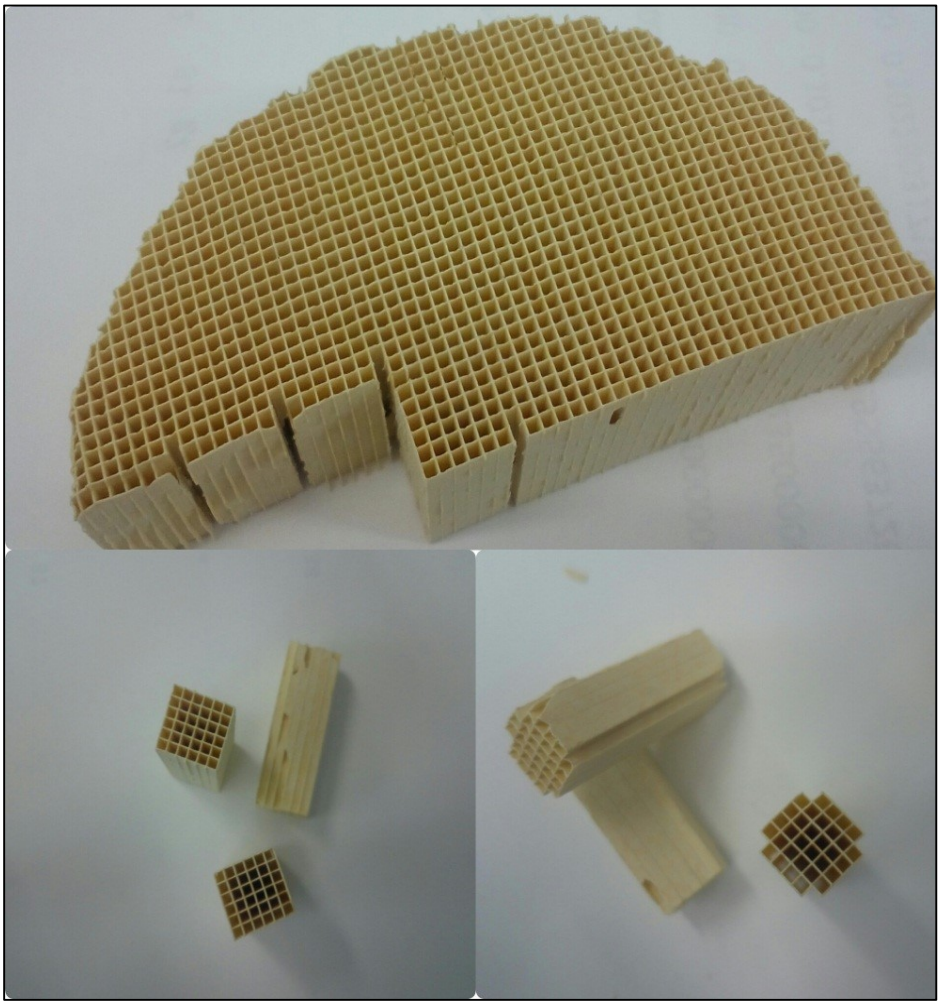

Figure 3.5. Cordierite monoliths used in this study.

In order to enhance surface area of the cordierites, they were wash-coated by colloidal silica solution for 40 min by using the Retsch UR1 ultrasonic mixer. Each monolith was

treated individually in order to observe the amount of the coated silica on their walls. In every 10 min, excess solution inside the channels was removed by injecting air with a syringe. This process prevents clogging the channels. After opening the channels, monoliths were dried at 180 W for 40 min and then, weighed again to obtain the coated weights. The schematic representation of this process is showed in Figure 3.6.

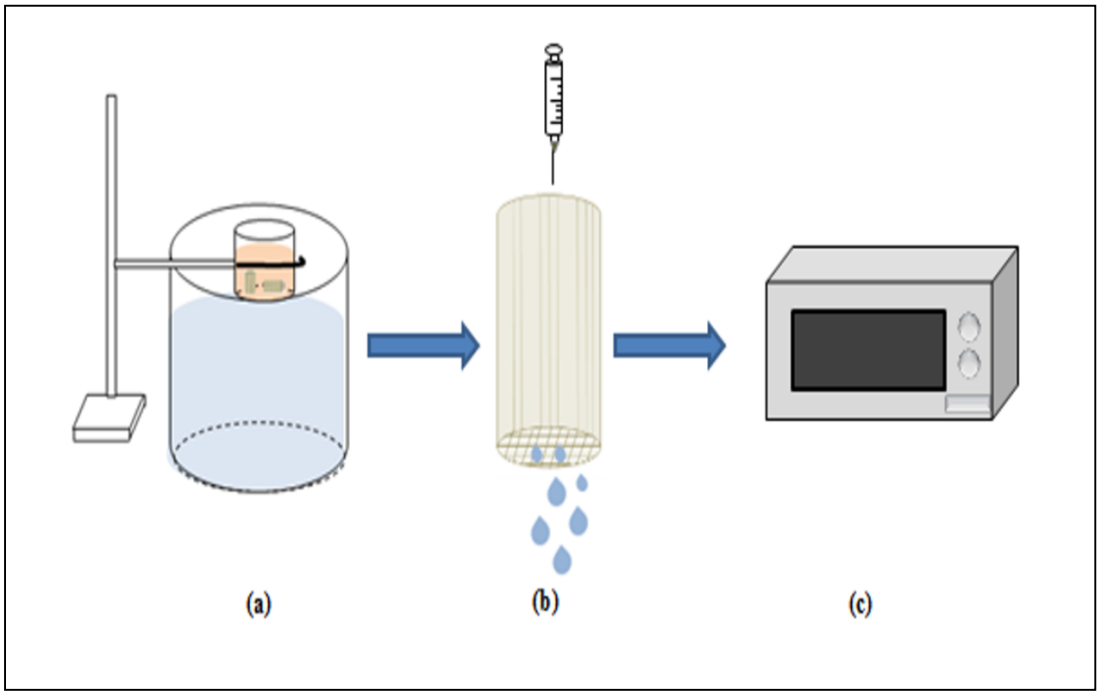

Figure 3.6. The process of the monolith coating system; (a) wash-coating in ultrasonic mixer, (b) removing excess solution through air by syringe, (c) dried in microwave.

The amount of the coated silica on the walls must be 0.15 g so that two monoliths can be used for one experiment. Based on the coated silica, the amount of $Mn(NO_3)_2$ tetrahydrate was calculated and dissolved deionized water at 85 °C. Afterwards, 2 wt.% Mn solution is filled into a syringe and injected through every channels drop by drop. In order to obtain a homogeneous dispersion, 2 wt.% Mn coated cordierite was mixed by using the Retsch UR1 ultrasonic mixer for 30 min and then, dried in the oven at 130 °C for 5 h.

In the end of 5 h, the monoliths must be cooled in the desiccator before injecting the Na_2WO_4 dihydrate, otherwise deterioration of Na_2WO_4 can be observed on the surface of

the cordierite monolith. After that, Na_2WO_4 dihydrate was injected with using the same procedure as Mn impregnation, then 2 wt.% Mn and 5 wt.% Na_2WO_4 coated cordierites were dried at 130 °C overnight. Finally, they were calcined at 800 °C for 8 h. Figure 3.7 shows the changes on the monoliths during the preparation process.

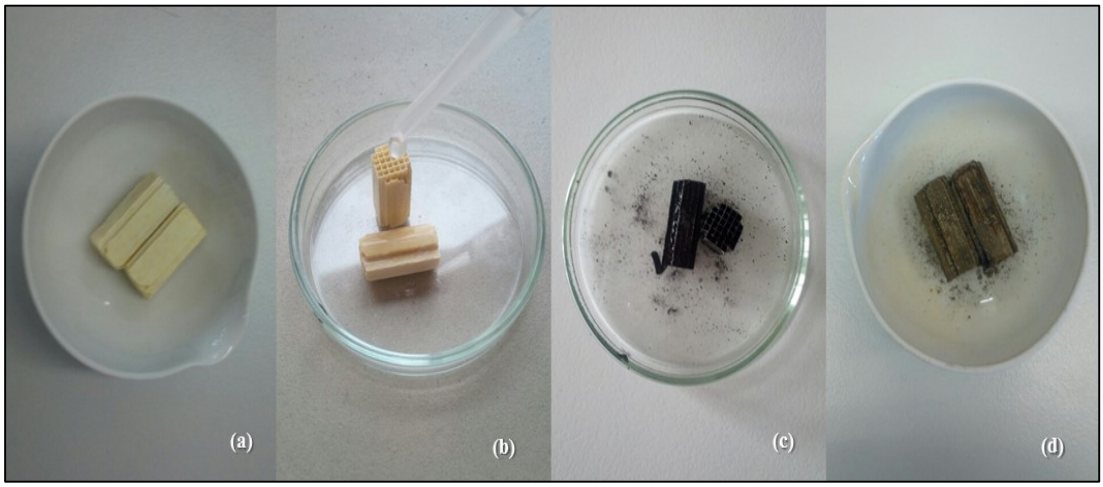

Figure 3.7. The alteration of the cordierite monolith during the preparation; (a) dried in over for 1 h after washing with acetone, (b) metal impregnation technique, (c) dried at 130 °C overnight, (d) after calcination at 800 °C.

3.2. Experimental System

In this study, catalytic reaction system shown in Figure 3.8 was designed and constructed in the Catalysis and Reaction Engineering Laboratory of Chemical Engineering Department of Boğaziçi University. The system consists of 1/4", 1/8" and 1/16" OD stainless steel and copper tubing, valves with stainless steel and brass fittings for gaseous species. High purity reaction gases were connected to the system and adjusted to a set point with using mass flow controller units. The desired amount of gases were mixed and sent to the by-pass line for the feed analysis or to the reactor for the product tests by using a two-way valve.

The temperature in the reactor was controlled by using a Shimaden FP21 programmable controller, which was attached to a K-type thermocouple to conduct the

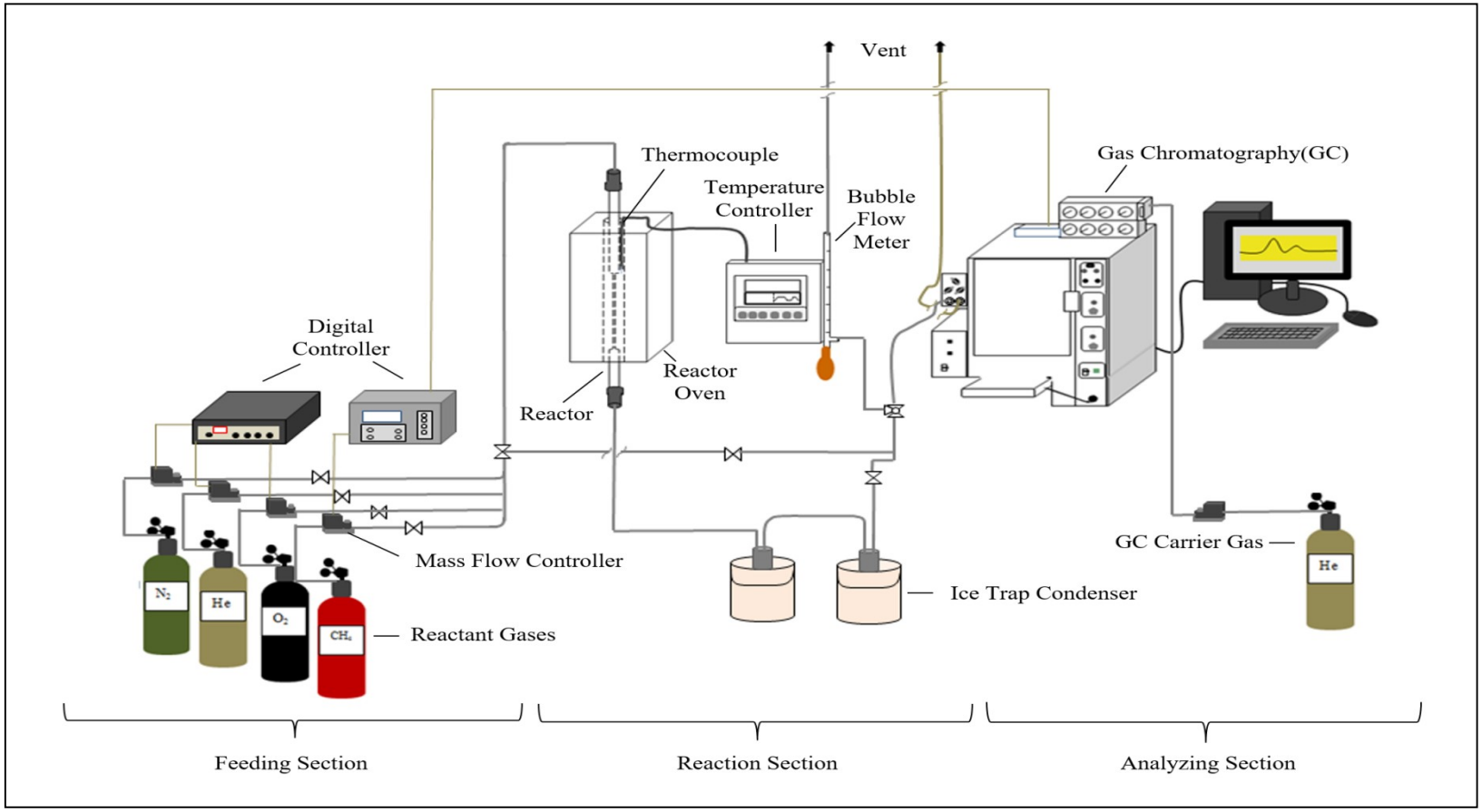

Figure 3.8. A schematic representation of the reaction system used in this study.

temperature inside the furnace. Before product gases reached to the analyze unit, they were passed through two series of condenser which can hamper any liquid products to keep GC columns from any possible damage. A bubble flow meter was provided exactly before the GC to check leakage and do calibration for mass flow controllers.

For all experiments, 4% nitrogen was used as an internal standard to evaluate volume shrinkage and assist to verify the percent of the product gases. Each analysis in the GC took 50 min; 29 min for analysis of the product gases and 21 min for cooling GC to its initial temperature.

3.2.1. Mass Flow Controller

The flow rates of high purity reaction gases were regulated by using two different types of digital controller. Each gas from pressurized cylinders passed through individual MFC, which is adjusted to the desired set point. Omega Model 7878 digital mass flow controllers were linked to the oxygen, nitrogen and inert helium tubes in order to control the flow of the gases. On the other hand, the GC He and methane gases were delivered to the system with Brooks 5850E mass flow controllers.

In order to calibrate the MFCs, a bubble flow meter connected to the system was used. Each gas was sent to the system with a known percentage at least for 10 min. After the gas flow was stabilized, the duration for the movement of the bubble between two points was measured. Therefore, for each real value of the flow rate a set value was obtained. For oxygen and nitrogen, only a narrow range of flowrates (2-20 $ml.min^{-1}$ for oxygen, 2-10 $ml.min^{-1}$ for nitrogen) was considered in calibration since higher values (20-80 $ml.min^{-1}$ for oxygen, 10-60 $ml.min^{-1}$ for nitrogen) could not be used due to the overlap of the peaks in Gas Chromatography.

3.2.2. Gas Chromatography

In order to analyze the feed or product gases, a Shimadzu GC 14A type gas chromatograph equipped with a Thermal Conductivity Detector (TCD) was used. The specifications of the gas analyzer are listed in Table 3.3.

Helium was used as a carrier gas for the GC while nitrogen was chosen as an internal standard to count the volume change during reaction. However, nitrogen and oxygen peaks overlapped and this may cause big errors for the calculation of the selectivity and yield of the product gases. In order to separate these two peaks from each other, a GC oven heating program, which was developed by Nadjafi (2015) was used; the column temperature was kept constant at 40 °C for 5 min period and then increased with an increment rate of 20 °C.min^{-1} to reach final temperature of 220 °C for 15 min. With this GC program, oxygen and nitrogen peaks could be separated as it can be seen in Figure 3.9.

Table 3.3. The specifications of the Gas Chromatography.

GC	**Shimadzu GC 14A**
Carrier gas	Helium
Carrier gas flow rate	30 ml.min^{-1}
Column final temperature	220 °C
Column final time	15 min
Column injection temperature	220 °C
Column initial temperature	40 °C
Column initial time	5 min
Column temperature increment rate	20 °C.min^{-1}
Column length & ID	6 m, 2mm ID, 1/8 inch OD
Column type	CBXN-1000 60/80
Detector temperature	230 °C
Detector type	TCD
Sample loop	2 mL
Sampling rate	100 ms

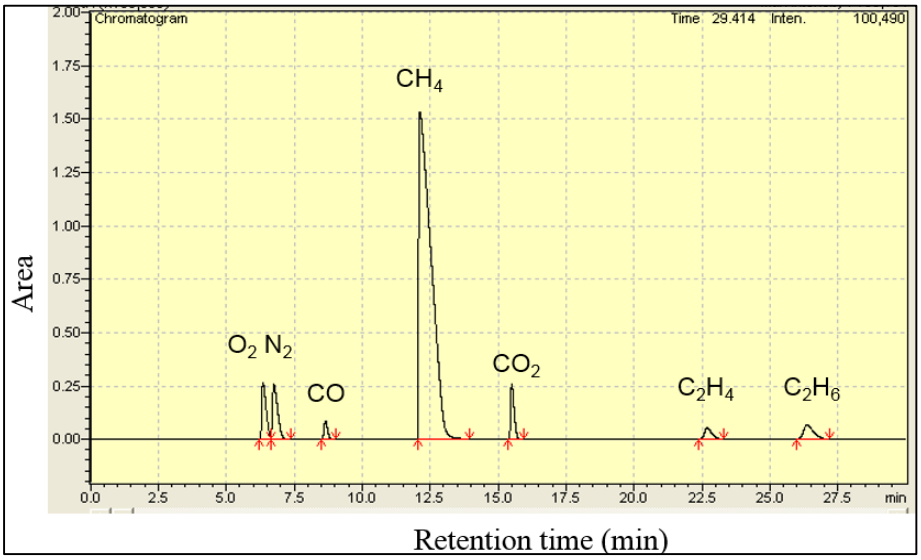

Figure 3.9. The location of the peaks after adjusting GC program.

3.2.3. Furnace and Temperature Controller

30 mm in diameter and 480 mm in length tubular electric furnace working with a temperature range 25-1000 °C was used for this study. A Shimaden FP-21 programmable controller was connected to the furnace. To heat up the furnace, a K-type thermocouple (Chromel (95% nickel, 2% manganese, 2% aluminum and 1% silicon), Alumel (95% nickel, 2% manganese, 2% aluminum and 1% silicon)) with a melting point of 1400 °C was attached to the controller. Thermocouple was inserted into the furnace and placed outside of reactor at the level of the catalyst. Since the length of the reactor was longer than the furnace upper and lower part of the reactor was in contact with the room temperature. Therefore, the upper part of the reactor was insulated with quartz wool, which was covered with aluminum foil. However, the lower part was kept without insulation. This procedure was always applied in order to prevent conversion of the desired product to by-product.

3.2.4. Catalytic Reaction System

For the experiments, a 10 mm in diameter and 810 mm in length packed-bed downward tubular reactor was used. Reactor was made of quartz in order to endure high temperatures. The diameter of the reactor was reduced to 2 mm right after the catalyst bed

to accelerate the flow of the product gases at the high temperature zone so that no more by-product converted from the desired one. Moreover, our previous experience had shown that this type of reactors enabled to increase C_2 selectivity noticeably although no appreciable changes on CH_4 conversion (Düşova, 2014).

To prepare the reactor for the reaction, firstly, lower part of the reactor was closed with quartz wool and 1-2 mm quartz chips were filled. To stabilize the quartz chips at that location, quartz wool was inserted again. The lower part of the reactor was covered such a way in order to reduce the dead volume. Then, the reduced diameter part of the reactor was filled with 0.63-1 mm quartz chips. Later, the specific amount of the catalyst was weighed which was 300 mg for particulate catalyst, 2 pieces for monolith or 300 mg for monosil. Upper and lower part of the catalyst bed was covered with quartz wool in order to prevent from any contamination and mixing with quartz chips. Lastly, 1-2 mm quartz chips were inserted into the above thicker part of the reactor with the same height of the reduced part. The schematic representation of the reactor preparation showed in Figure 3.9 and the close images of the different catalyst bed in the reactor demonstrated in Figure 3.10.

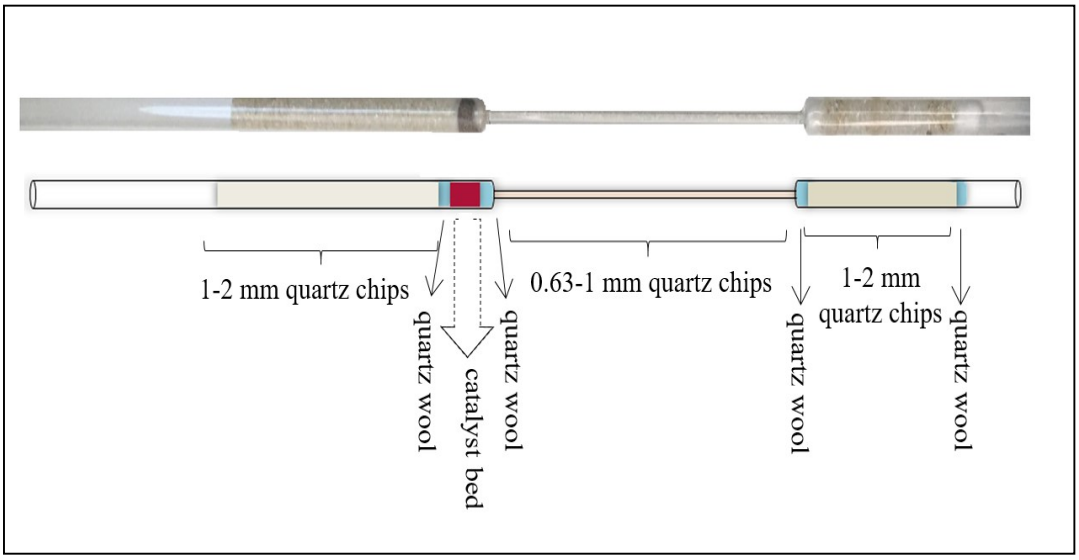

Figure 3.10. Schematic representation of the reactor filling procedure.

In this experiments, the quartz chips was used as filling material to decrease the temperature gradient in the catalyst bed and minimize the contribution of gas phase

reactions that decompose products. The quartz chips were obtained from the quartz glasses. These quartz glasses were crushed and sieved. Then, they were separated according to their size. Finally, they were washed by hydrochloric acid and acetone. At the end of the each experiment, used quartz chips was treated with acetone and distilled water and dried in the oven before keeping for the next catalytic run.

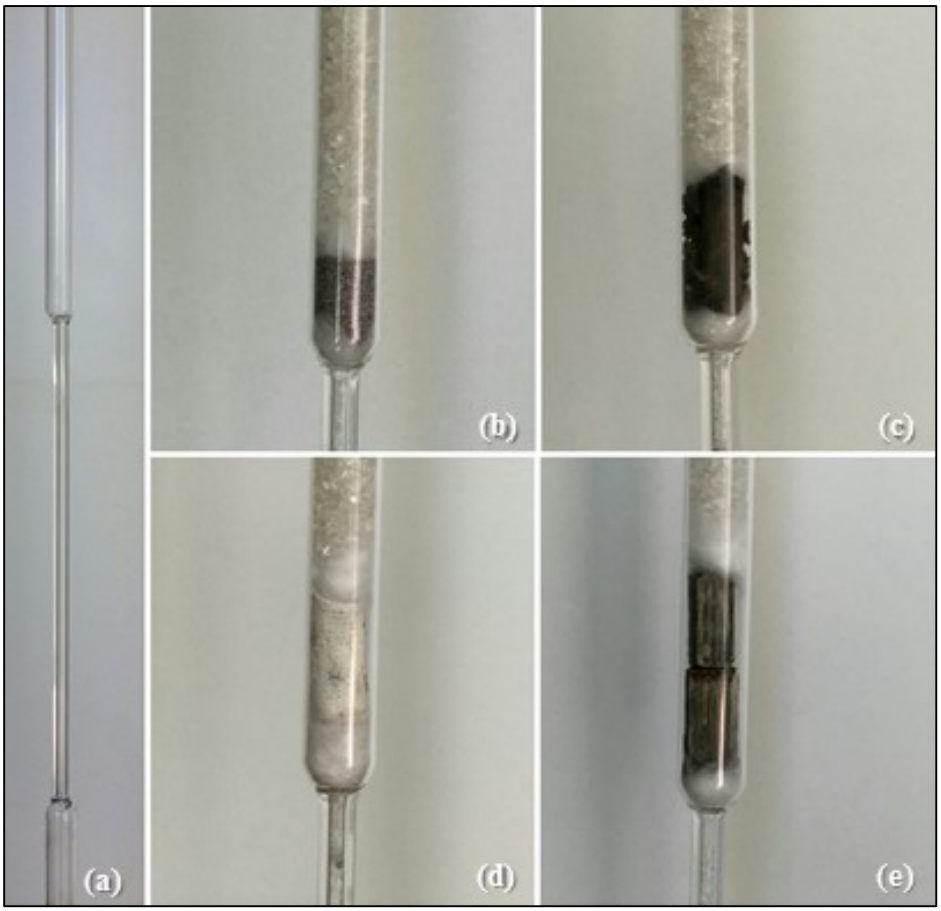

Figure 3.11. Different catalyst types in reactor; (a) empty reactor, (b) particulate catalyst bed, (c) monosil, (d) monosil with Mn, (e) cordierite monolith.

At the beginning of each test, a feed analysis was done to examine the accuracy of the feeding gases and to use for the calculations of the product gases. The percentage of the nitrogen was always taken 4% as an internal standard. Thereby, the amount of each reactant (methane and oxygen) was calculated based on 96% part of the feed. Before the feed analysis, gases were mixed for 15 min in order to obtain an accurate result. After that, temperature controller was set to the desired temperature. Heating of the reactor took 50

min by passing through 5 $ml.min^{-1}$ nitrogen. After reaching the desired temperature, first methane then oxygen was sent to the system at the reaction conditions. The reactants were mixed for 20 min, and then first data was taken for period of 29 min. After 21 min cooling, GC became ready for the next data by flashing the ready lamp on the GC keyboard.

Besides comparing the different type of catalyst preparation, the temperature dependence was also investigated at the reaction temperature of 600, 650, 700, 725, 750, 800, 815, and 860 °C for particulate catalyst and monolithic catalyst like monosil and cordierite monolith. During all tests, total flow rate was taken as 120 $ml.min^{-1}$ and different CH_4/O_2 ratios was tested. Furthermore, different heating process of the reactor was compared each other.

In all cases output flow rate, selectivity, yield and conversion were calculated according to our previous experiments (Nadjafi, 2015).

$$F_{out}=\frac{X_{N_{2in}}\times F_{in}}{X_{N_{2out}}} \tag{3.3}$$

$$\text{Conversion}=\frac{X_{CH_{4in}}\times F_{in}-X_{CH_{4out}}\times F_{out}}{X_{CH_{4in}}\times F_{in}} \tag{3.4}$$

$$\text{Selectivity}=\frac{2\times F_{out}(X_{C_2H_4}+X_{C_2H_6})}{X_{CH_{4in}}\times F_{in}-X_{CH_{4out}}\times F_{out}} \tag{3.5}$$

$$\text{Yield}=\text{Selectivity}\times\text{Conversion} \tag{3.6}$$

4. RESULTS AND DISCUSSION

$Mn/Na_2WO_4/SiO_2$ catalysts in different forms were prepared to investigate the performance of the oxidative coupling of methane reaction in a micro-structured packed bed reactor. Total flow of 120 $ml.min^{-1}$ and 300 mg 2 wt.% Mn 5 wt.% Na_2WO_4/SiO_2 catalyst were used for each experiment. 810 mm length and 10 mm ID quartz reactor with a reduced diameter of 2 mm right after the catalyst bed was utilized by filling the dead volume of the reactor with quartz chips with different size in order to prevent the non-catalyzed gas phase reactions.

4.1. Oxidative Coupling of Methane Reaction over Different Catalyst Forms

Three $Mn/Na_2WO_4/SiO_2$ catalyst forms (particulate, monolith and monosil) were tested for their OCM performance. The results of these three forms were presented and discussed in the following sections.

4.1.1. Reaction Tests with Particulate Catalyst

Particulate catalyst prepared by incipient to wetness impregnation method was tested by changing the temperature and feed compositions of the reaction.

4.1.1.1. Effect of the Temperature Variations. 45-60 mesh size of $Mn/Na_2WO_4/SiO_2$ particulate catalyst was tested under the temperature range of 600-860 °C. When the reactor furnace reached the desired temperature, the feed gas was introduced and mixed for 20 min before the first data was taken. Then the temperature was increased to the next level; the same sampling procedure was applied for each temperature increments.

The first experiment was carried out at the CH_4/O_2 ratio of 5. At the beginning of the experiment (at 600-650 °C), there was no change in selectivity and yield. This indicates that OCM reaction is not favorable at low temperatures. When the catalyst bed reached to 700 °C, the rapid enhancements were observed in conversion, selectivity and yield. At this

temperature, the water formation at the outlet of the reactor was also observed showing that ethylene production started to increase. A particular amount of the steam was condensed at the outlet of the reactor due to the fast transition from the high temperature to the room temperature (Figure 4.1).

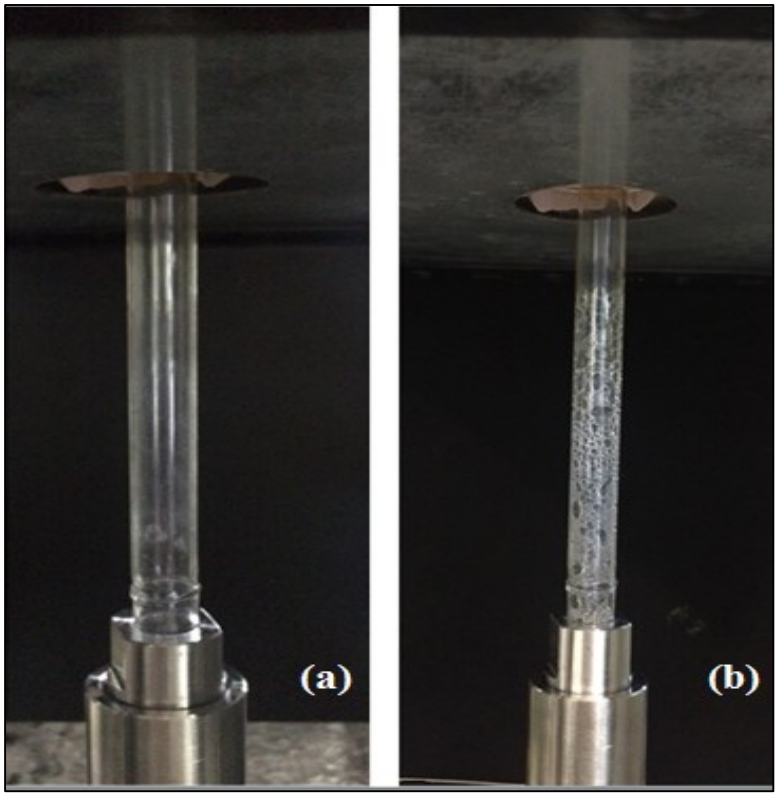

Figure 4.1. The outlet of the reactor; (a) before the reaction, (b) after the reaction.

The uncondensed steam was trapped in the condensers before the product gas entering the GC equipment. This phenomena was also observed by several researchers (Farsi *et al.,* 2011; Mleczko *et al*., 1997; Schomäcker *et al.,* 2013). In the study of Farsi and co-workers (2011) and Alavi and Shahri (2009), they claimed that water first came from the ethane formation as shown in Equation (4.1), then the ethylene formation reaction by using the formed ethane which is showed in Equation (4.2).

$$2CH_4 + 0.5O_2 \rightarrow C_2H_6 + H_2O \quad (4.1)$$

$$C_2H_6 + 0.5O_2 \rightarrow C_2H_4 + H_2O \quad (4.2)$$

After the temperature started to increase from 650 to 700 °C, the water formation was observed at the outlet of the reactor.

The yield reached to the maximum at temperature range of 700-750 °C as shown in Figure 4.2, after that the decline was observed for not only yield but also selectivity. Therefore, it can be deduced 725 °C is the optimum temperature for the OCM reaction over the particulate catalyst when the CH_4/O_2 ratio is 5.

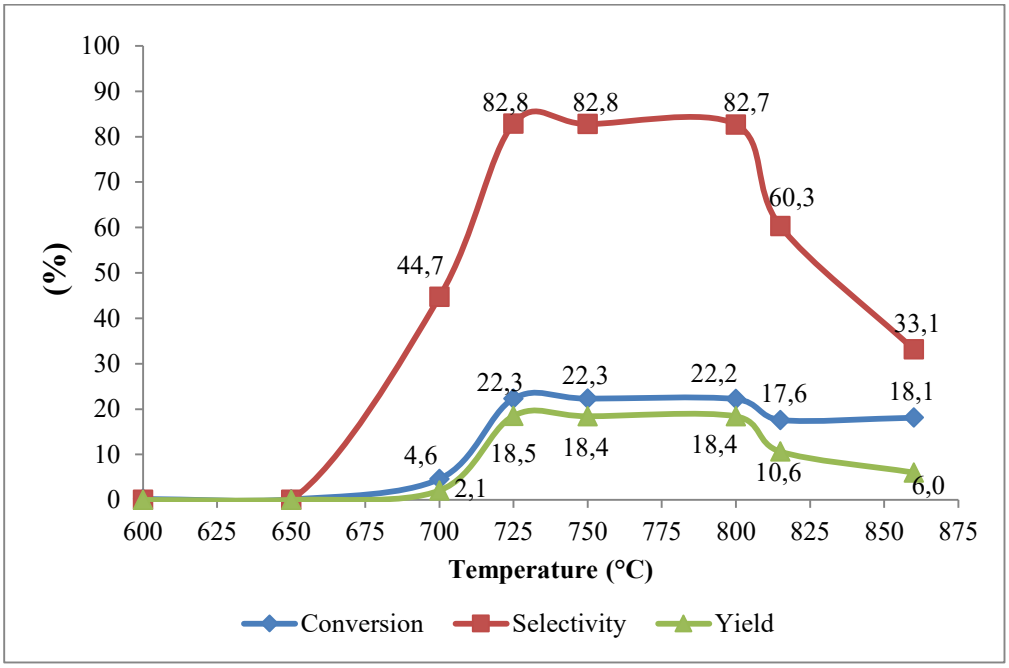

Figure 4.2. Influence of the temperature over the particulate catalyst when CH_4/O_2=5.

The temperatures between 750-860 °C were not favorable for OCM reaction as shown in Figure 4.2. Although there was no significant change of conversion, C_{2+} yield and selectivity started to decrease slowly. The methane conversion remained the same because CO formation increased dramatically. The gas phase reactions might start to dominate the system as it was also observed by Farsi *et al.* (2011). They indicated that the desired product ethylene started to convert into carbon monoxide and hydrogen as shown in Equation 4.3.

$$C_2H_4 + 2H_2O \rightarrow 2CO + 4H_2 \qquad (4.3)$$

When temperature reached 815 °C, H_2 formation was detected with a high percentage of CO.

4.1.1.2. Effect of the Feed Gas Composition. Particulate catalyst was also tested at different feed gas compositions in order to find out the best methane to oxygen ratio. The experiments were performed at CH_4/O_2 ratio of 4.3, 5, 7 and 10. The comparison of the results obtained at various ratios was given in Figure 4.3 at 725 °C, which was determined as the best temperature.

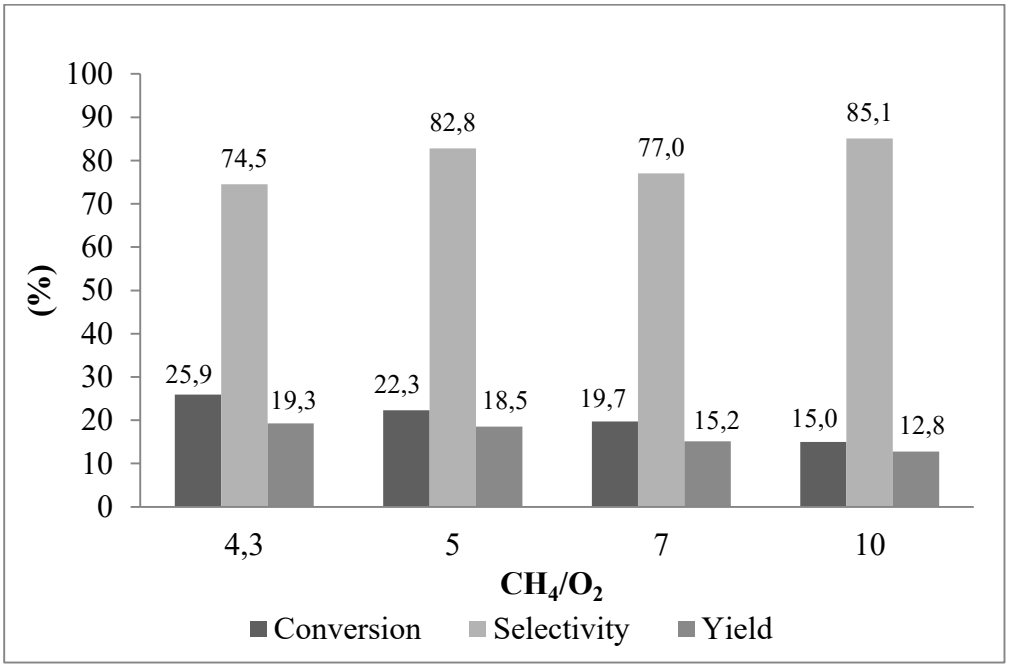

Figure 4.3. The effect of methane to oxygen ratio at 725 °C, particulate catalyst.

The results in Figure 4.3 indicate that OCM reaction is favored at low CH_4/O_2 ratios. When the ratio was 4.3, the highest yield and conversion was obtained. However, the gas phase side reactions (CO_x formation) became also dominant at lower ratios. Especially, when the methane to oxygen ratio decreased from five to lower values, the undesired by-product increased significantly compared to slight increment of yield and conversion. The increase of yield is related to the oxygen amount in the feed gas. Since the oxygen amount increased with decreasing the CH_4/O_2 ratio, more lattice oxygen became available on the

surface of the catalyst. Thereby, ethane and ethylene formation increased as well as the CO_x.

Figure 4.4 and 4.5 show the performance of particulate catalyst at different temperatures when the CH_4/O_2 ratios were 7 and 10 respectively.

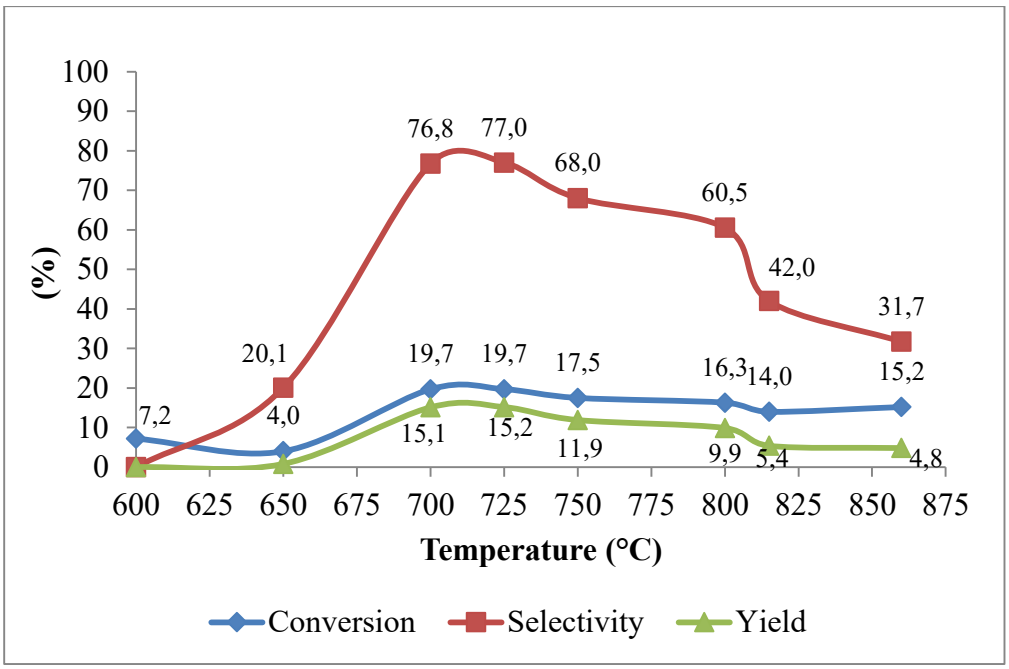

Figures 4.4. The result of particulate catalyst at different temperatures when CH_4/O_2=7.

At the CH_4/O_2 ratio of 7, a slower increment of conversion, selectivity and yield was observed with increasing temperature compared to the higher CH_4/O_2 ratios. The optimum temperature was again around 725 °C. However, the maximum yield range narrowed between 700-725 °C.

Figure 4.5 shows the results obtained at the CH_4/O_2 ratio 10, which exhibits much lower C_{2+} selectivity than the results obtained at the ratios of 5 and 7. Apparently, the methane was converted to CO_x by products, as it is evident from the fact that the oxygen gas in the feed was depleted. This was also observed by other investigators (Yaghobi *et al.,* 2013; Baiker *et al*., 2014).

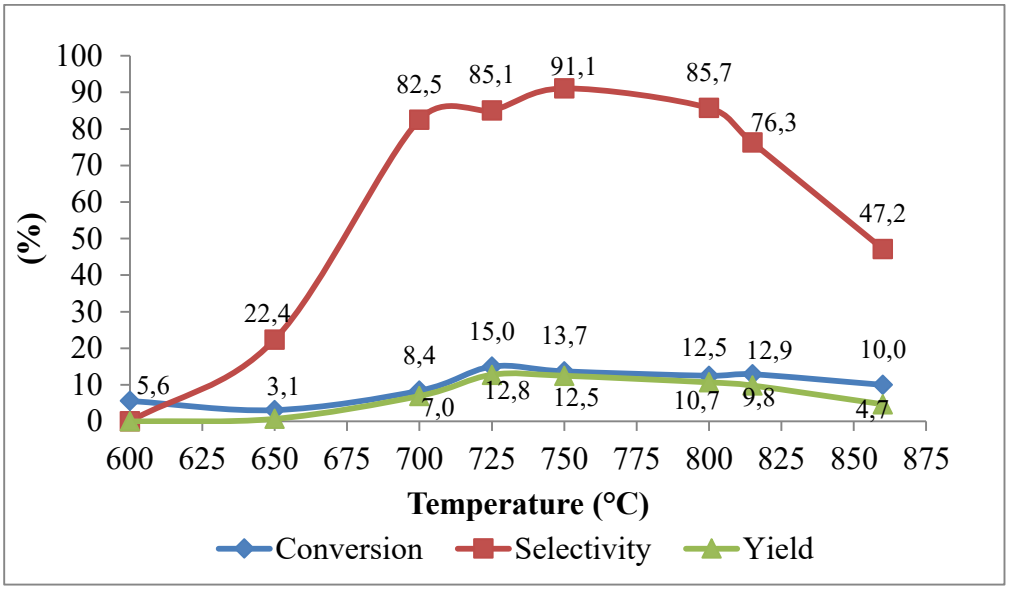

Figure 4.5. The result of particulate catalyst at different temperatures at CH_4/O_2=10.

4.1.2. Reaction Tests with Monosil

4.1.2.1. Comparison of Different Monosil Preparation. As explained in Section 3.2.2.2, three different monosil preparation procedures were performed (regular formation, addition of manganese in advance and addition of C_{16}TAB (MCM-41 Monosil).

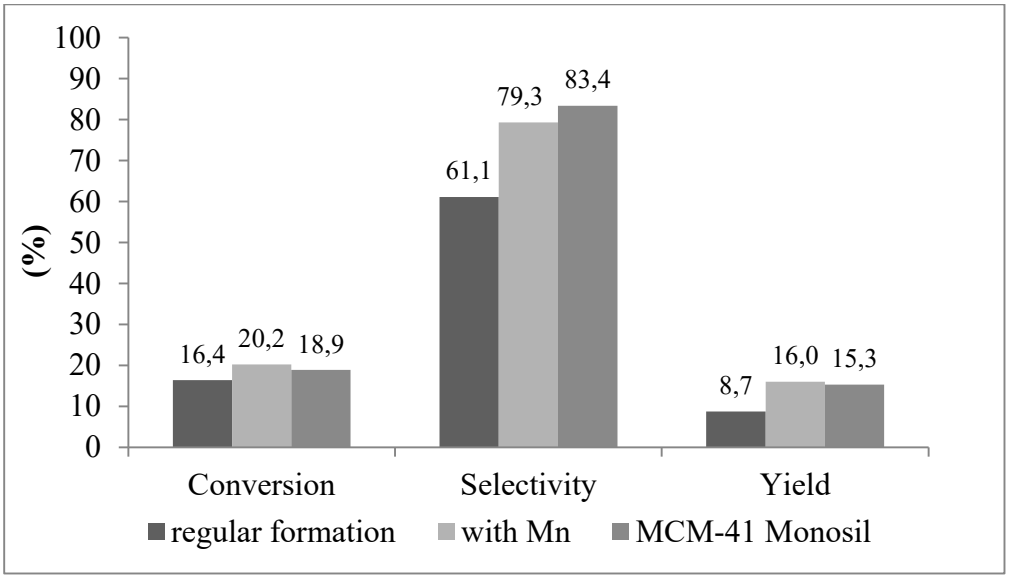

Figure 4.6. Comparison of different monosil formation when CH_4/O_2=5 at 725 °C.

Those monosil types were tested and compared at 725 °C under the CH_4/O_2 ratio of 5. Figure 4.6 shows that the best result was obtained by using monosil with manganese for the reaction.

4.1.2.2. Effect of Calcination Procedure for Monosil with Mn. In this section, the experiment was done with monosil prepared by manganese addition during sol preparation, which was mentioned Section 3.2.2.2. The calcination step was performed with two different ways. Firstly, monosil was calcined in reactor furnace for 8 h at 800 °C with a ramp rate 1 °C/min under the flow of dry air. Afterwards, the reaction was carried out at that temperature in order to inhibit any negative effect. Secondly, calcination was performed in muffle furnace at 800 °C with a ramp rate of 1 °C/min. The comparison of the results for both methods exhibited in Table 4.1.

Table 4.1. The Comparison of the different calcination steps of monosil at 800 °C.

Calcination Method	**CH_4 Conversion**	**C_{2+} Selectivity**	**C_{2+} Yield**
Calcination in reactor furnace	12.5	67.5	8.4
Calcination in muffle furnace	12.1	85.7	10.7

The results shown in Table 4.1 indicate that calcination in muffle furnace is more favorable. Therefore, the following experiments were done with monosil calcined in muffle furnace.

4.1.2.3. Effect of Reaction Temperature. Experiments with monosil were performed at 600-860 °C. The results for CH_4/O_2 ratio of 5 at different temperatures were demonstrated in Figure 4.7.

After the reactor furnace reached the 600 °C, a data was taken. Negligible amounts of ethane and ethylene was detected indicating that OCM reaction was not favorable over monosil at this temperature. At 650 °C H_2O formation was observed at the outlet of the

reactor which was a sign of the enhancement of ethylene production (Farsi *et al.*, 2011) as it is evident from Figure 4.7. Although the reaction started at lower temperature, the optimum temperature was the same; however, the yield remained well below the particulate catalyst. Nevertheless, these results were encouraging for the further studies over the monosil.

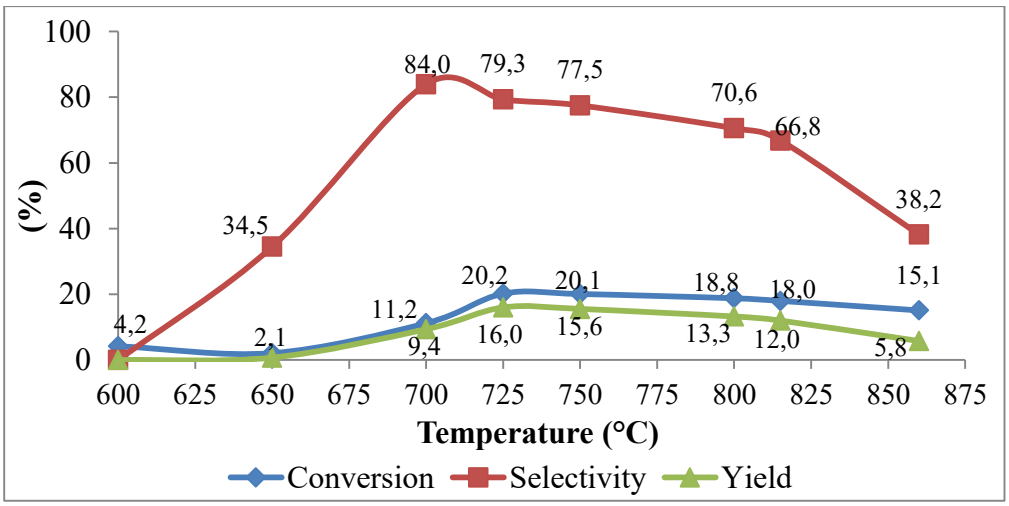

Figure 4.7. Effect of the temperature over the monosil with Mn at CH_4/O_2=5.

4.1.2.4. Effect of the Feed Gas Composition. Monosil with manganese was tested at different methane to oxygen ratios in order to determine the performance of this catalyst under different conditions.

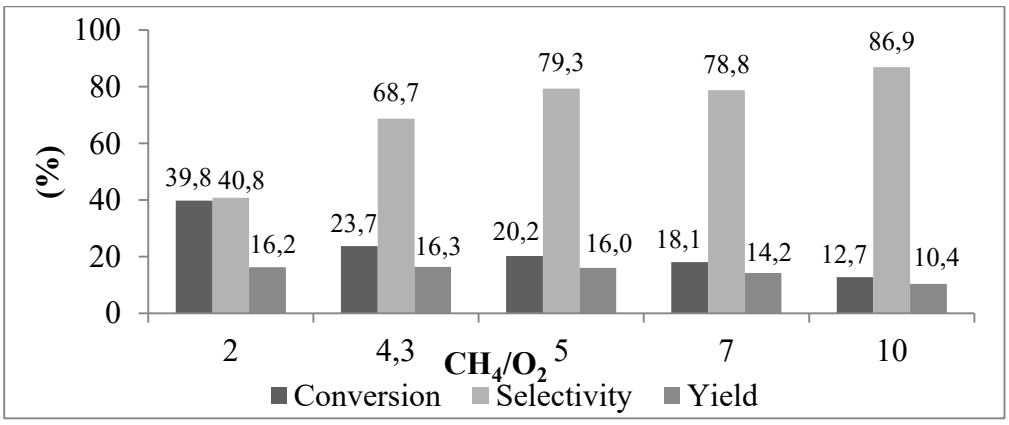

Figure 4.8. The effect of methane to oxygen ratio at 725 °C for monosil.

A summary of results, which contained the works under the CH_4/O_2 ratios of 2, 4.3, 5, 7 and 10, was shown in Figure 4.8.

The relations similar to those for the particulate catalyst were also obtained among the methane to oxygen ratio, and yield, selectivity and conversion over the monosil catalyst. The lower value of CH_4/O_2 ratio was more favorable. However, especially the CH_4/O_2 ratio was decreased below 5 (for example at 4.3 and 2), conversion continued to increase while yield and selectivity decreased. This may be again attributed to CO_x formation.

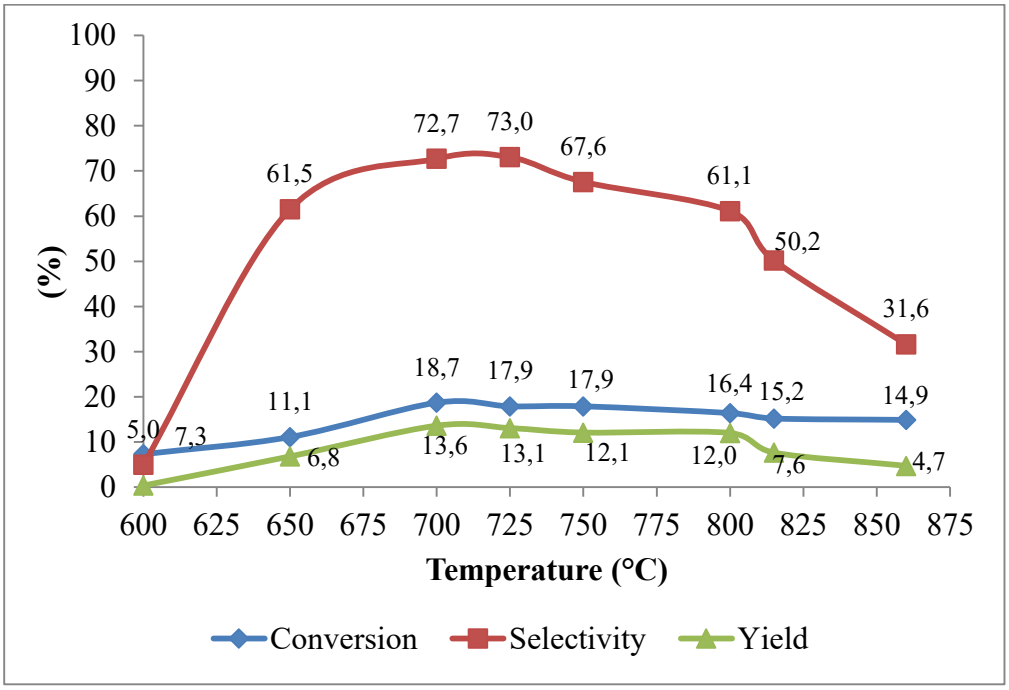

Figure 4.9. The result of monosil at different temperatures when CH_4/O_2=7.

The results of CH_4/O_2 of 7 and 10 were also examined at different temperatures shown in Figures 4.9 and 4.10, respectively.

The selectivity started to increase when the CH_4/O_2 ratio was 7 after 700 °C (Figure 4.9) while it continued to be high at even higher temperatures at the CH_4/O_2 ratio of 10 (Figure 4.10). However, the conversion was much higher at the CH_4/O_2 ratio of 5, making this ratio more appropriate for high yield.

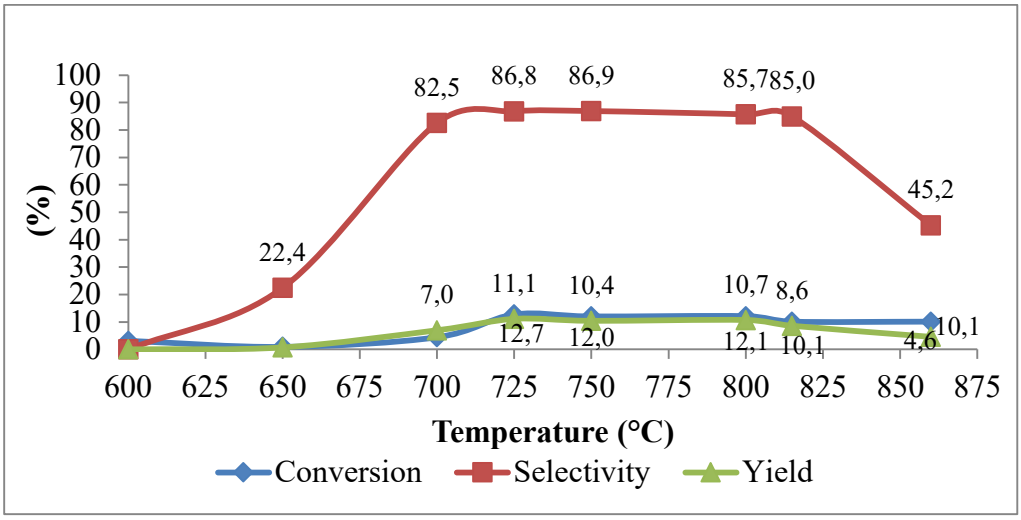

Figure 4.10. The result of monosil at different temperatures when CH_4/O_2=10.

4.1.3. Reaction Tests with Cordierite Monolith

The performance of the OCM reaction was also investigated using a commercial cordierite monolith as a support for 2 wt.% Mn and 5 wt.% Na_2WO_4 catalyst. In order to compare with other catalyst preparation methods, the experiment for cordierite monolith was also carried out under the same conditions as the other two forms.

4.1.2.1. Effect of Reaction Temperature. The first cordierite monolith experiments were carried out at CH_4/O_2 of 7 by examining the influence of the temperature enhancement. The results for this experiment were shown in Figure 4.11.

The OCM performance of the catalyst over the cordierite support differed significantly from the particulate catalyst and monosil. For example, the catalyst did not activate at 700 °C. Consequently, negligible amount of C_{2+} yield was observed. The selectivity, yield and conversion continued to increase throughout the temperature increment. However, the performance was still much lower than that obtained over the particulate and monosil catalysts even at the high temperatures. In fact, the yield started to decrease after 800 °C indicating that this form of support may not be suitable for OCM process.

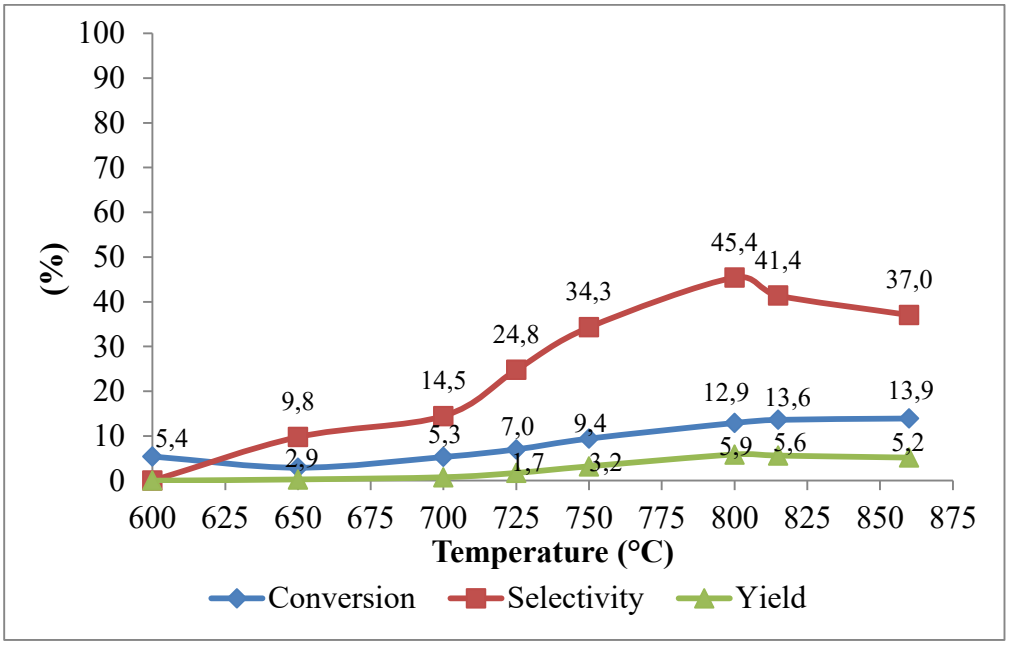

Figure 4.11. Influence of the temperature over the cordierite monolith when CH_4/O_2 =7.

4.1.2.1. Effect of Feed Gas Comparison. With the hope to eliminate the negative effect of cordierite monolith, the feed gas composition was changed from 7 to 5 as shown in Figure 4.12 and 4.13, respectively.

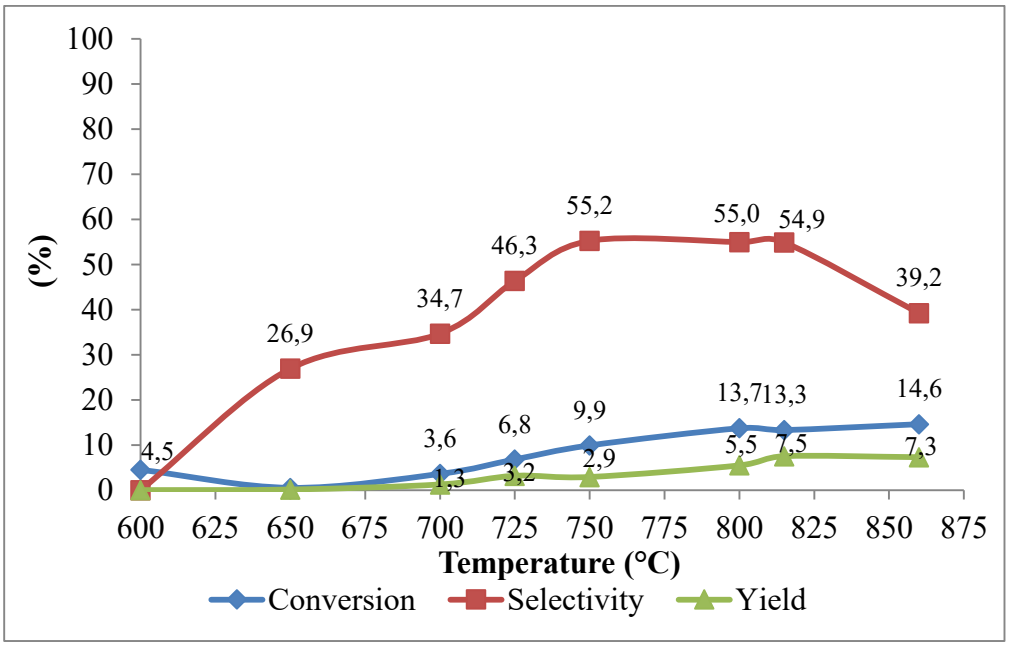

Figure 4.12. The result of cordierite monolith at different temperatures at CH_4/O_2=5.

After methane to oxygen ratio was decreased to 5 from 7, a slight improvement was observed for C_{2+} yield, but this was not comparable to those obtained with monosil and particulate catalyst. The most noticeable difference of the cordierite monolith from the two other formations was the increase of the yield with increasing of reaction temperature. However, this enhancement came to a halt at about 860 °C indicating that the most suitable temperature was shifted to the higher values for this support. One possible reason for this may be the poor heat transfer nature of cordierite monolith.

After testing these CH_4/O_2 ratios, it was deduced that cordierite monolith was not a good choice for the OCM reactions. The aggregated results at different CH_4/O_2 ratios (2, 4.3, 5, 7 and 10) exhibited in Figure 4.13 for all of them, cordierite monolith did not demonstrate a good performance. Still, the same relation with the higher oxygen amount and the increment of C_{2+} yield was observable even though the values were extremely low.

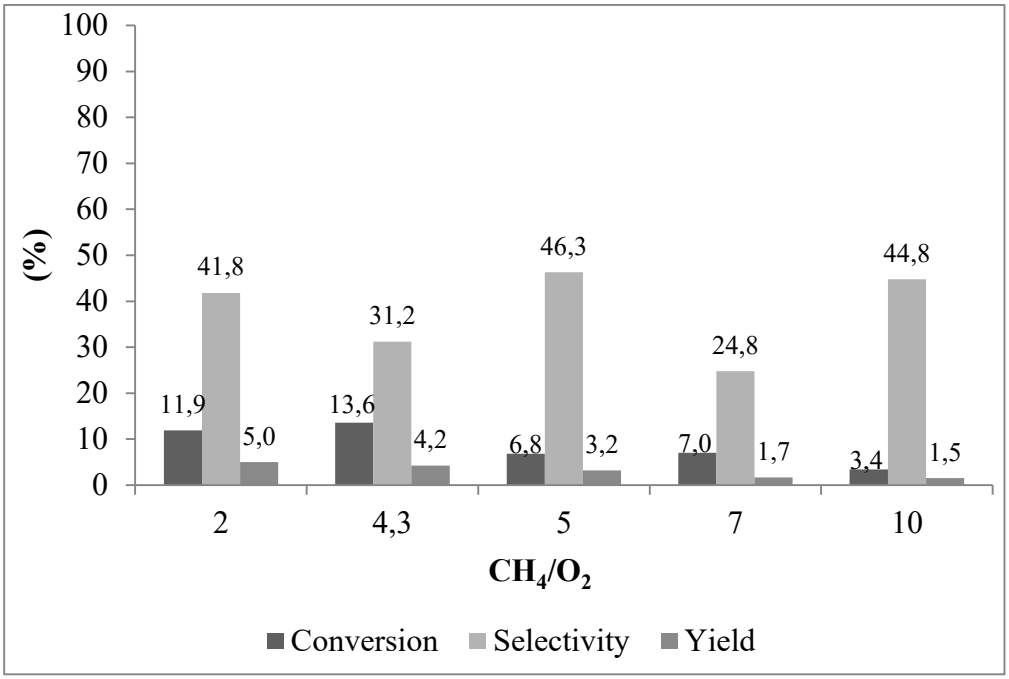

Figure 4.13. The effect of methane to oxygen ratio at 725 °C, cordierite monolith.

4.2. By-products Formation during OCM Process

The main by-products during the OCM reaction are carbon monoxide and carbon dioxide; the formation of these products (CO_x) was also investigated for the monosil and particulate catalyst tests. Figures 4.14 and 4.15 show the variations of CO_x formation for particulate catalyst and monosil, respectively at different CH_4/O_2 ratios.

The changes of CO_x formation at different values of CH_4/O_2 clearly show that CO_x formation is more favorable at lower ratios. The higher oxygen amount at the low ratios might be used for the CO_x formation (Alavi and Shahri, 2009).

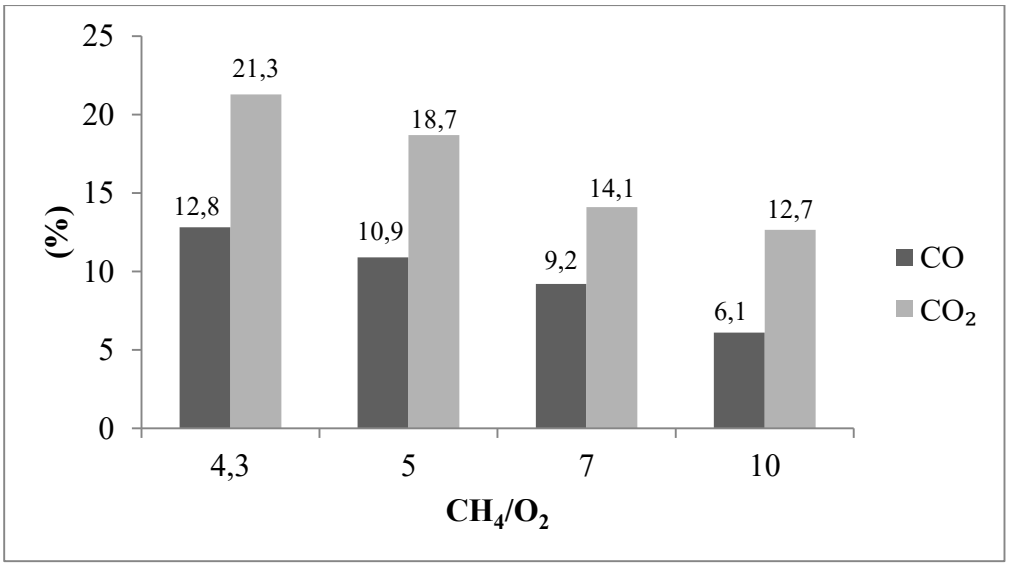

Figure 4.14. The CO_x alteration based on the CH_4/O_2 ratios for particulate at 725 °C.

Figure 4.14 also shows that CO_2 formation was always higher than CO formation at 725 °C. Farsi *et al.* (2010) claimed that CO converts to CO_2 due to available oxygen in the feed. The reaction of this formation was shown in Equation (4.4).

$$CO + 0.5O_2 \rightarrow CO_2 \qquad (4.4)$$

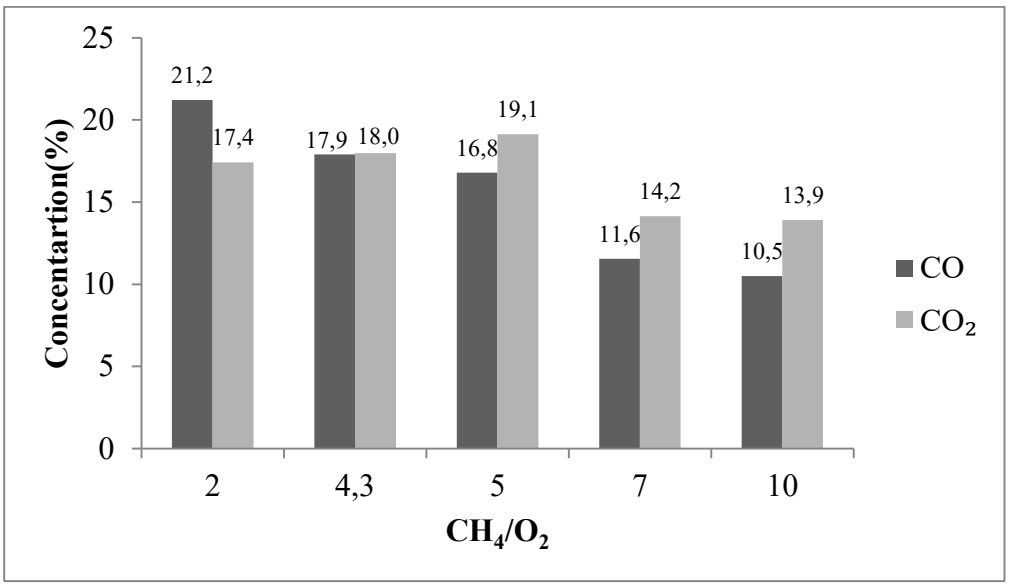

Figure 4.15. The alterations of CO according to the CH_4/O_2 ratios for monosil at 725 °C.

The same situation was also observable for monosil. However, in this case, the CO_x formation was a slightly higher.

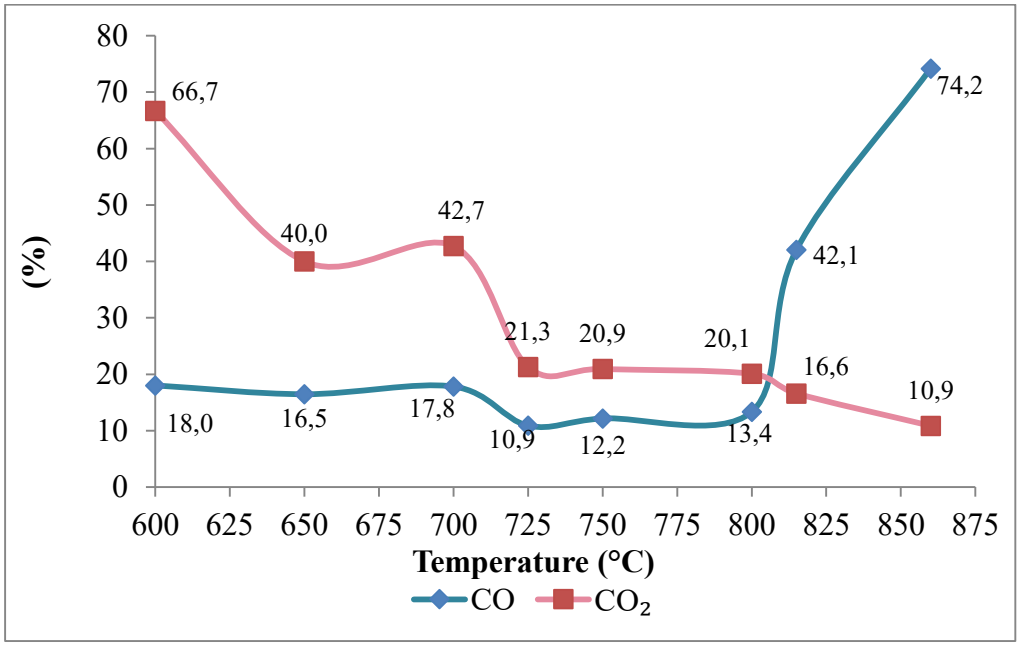

Figure 4.16. The temperature effect on the CO_x formation, particulate, when CH_4/O_2=5.

Another trend was observed when there was temperature increments during the OCM reaction; increasing temperature causes a decline of carbon dioxide whereas it leads to an increment for carbon monoxide. This can be observed clearly in Figure 4.16. This phenomenon was explained in two different ways in literature. Farsi *et al.* (2011) claimed that, at high temperatures, steam reforming of ethylene took place. This was also illustrated in Equation (4.3). On the other hand, some researchers deduced that the reverse water gas-shift reaction is the reason of CO increment at high temperatures, which converts the carbon dioxide into carbon monoxide, as shown in Equation (4.5) (Koirala *et al.*, 2014; Amin and Nikoo, 2011; Shahri and Pour, 2010).

$$CO_2 + H_2 \rightarrow CO + 2H_2O \quad (4.5)$$

Both phenomena might occur during the OCM reaction because the CO_2 and C_2H_4 production decreased while the CO and H_2O formation increased at high temperatures. Ethylene is a reactant for steam reforming reaction and CO is a product. This could be explained why the ethylene is declined. On the other hand, CO_2 is the main reactant for the reverse water gas shift reaction, whereas CO and H_2O are the products. Thus, because of these two reactions CO formation increased dramatically after 800 °C.

4.3. Comparison of Different Catalyst Preparation Methods

Three different catalyst forms were prepared and tested at the same conditions under OCM reaction. Among them particulate catalyst prepared by incipient to wetness impregnation method showed the best performance during the reaction. However, monosil showed very close results to particulate catalyst that makes it a promising route for the next catalyst preparation techniques. The worst results were obtained for cordierite monolith, which proved that cordierite is not suitable for the OCM reaction. The following figure shows a comparison of the three catalyst types.

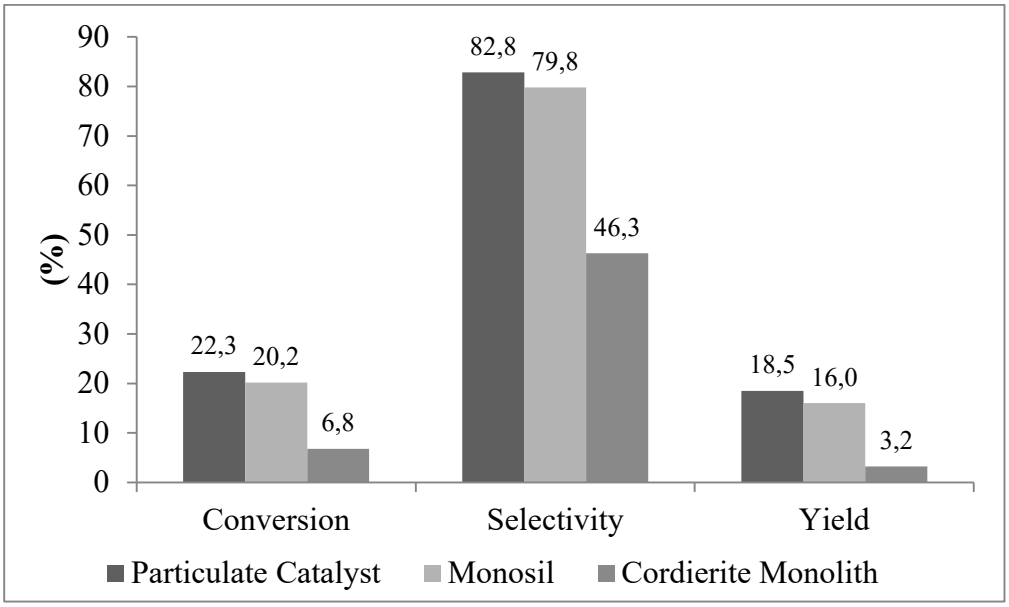

Figure 4.17. Comparison of catalyst types when CH_4/O_2=5 at 725 °C.

The results at 725 °C and CH_4/O_2 ratio of 5 shows that there is a small difference between particulate catalyst and monosil. Further modifications in monosil structure might provide a better catalyst structure for OCM reaction. Since the well-ordered macro- and mesopores of monosils allow an adequate diffusion of molecules into the active sites, this promotes a higher conversion.

4.4. Stability Tests for Monolithic Silica

The stability of the $Mn/Na_2WO_4/SiO_2$ catalyst was carried out by testing two different procedures. The first one was related to the time dependence. The OCM reaction of monosil was performed at 725 °C and methane to oxygen ratio of 10 for a 600 minute of reaction duration. The results demonstrate in Figure 4.18 below.

The results in Figure 4.18 show that monosil remained very stable for a 10 h period. Another indicator for the stability was the hysteresis test. As mentioned in experimental section, the reaction tests were started at low temperatures and then the temperature increased step by step taking sample at certain interval.

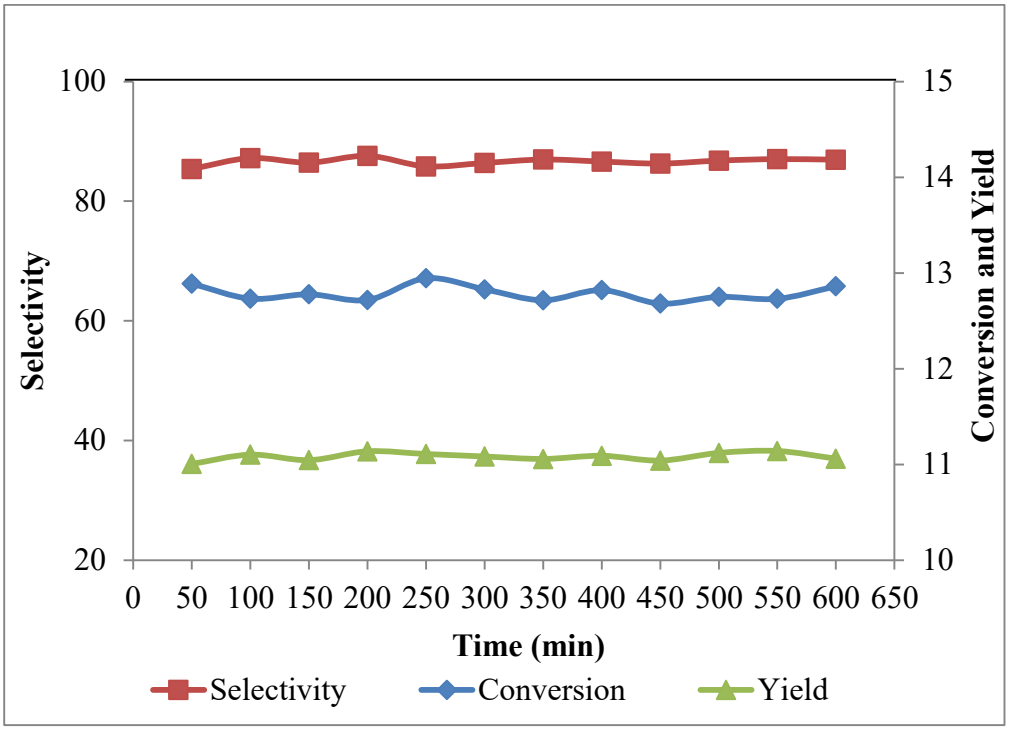

Figure 4.18. Stability results of monosil at 725 °C and CH_4/O_2 ratio of 10 for 10 h.

After the system reached to 860 °C in a standard experimental cycle (yield and selectivity were decreased with the increasing temperature), the temperature gradually decreased (with sampling at the interval again) until the initial temperature of 725 °C, the selectivity and yield were improved back and reached to the values quite close to the initial value obtained at 725 °C. The results were summarized in Table 4.2.

Table 4.2. The durability of the $Mn/Na_2WO_4/SiO_2$ catalyst at high temperatures and CH_4/O_2 ratio of 5.

Temperature (°C)	**Specification**	**Conversion (%)**	**Selectivity (%)**	**Yield (%)**
725	Temperature increment	20.2	79.3	16.0
860	Temperature increment	15.1	79.3	5.8
725	Temperature decline	23.7	72.7	16.3

4.5. Oxidative Coupling of Methane Reaction Test without Using Catalyst

The blank test was also carried out by replacing the catalyst with quartz chips in order to evaluate the true performance of the OCM reaction without $Mn/Na_2WO_4/SiO_2$ catalyst. The results are shown in Figure 4.19.

From Figure 4.19 it is obvious that the trend is the similar with the particulate catalyst discussed below Figure 4.2 and monosil in Figure 4.7, which is the best performance again in the range of 700-800 °C. However, yield and selectivity are considerably lower than the reactions carried out by particulate catalyst or monosil. This indicates that C-H bond activation in methane predominantly via catalytic routes to obtain C_{2+} products (Bhatia *et al.,* 2008).

The same tests was done by several researchers (Iglesia and Takanabe, 2009; Li *et al.,* 2006; Nadjafi, 2015). They all observed that reactions of the empty reactor always lead to the same result, which is a lower C_2H_6 selectivity. Iglesia and Takanabe (2009) claimed that the blank test reflects the slower formation of CH_3• radicals when catalyst surface is not present since the ethane formation takes place when two CH_3• radicals combined on the catalyst surface at first step.

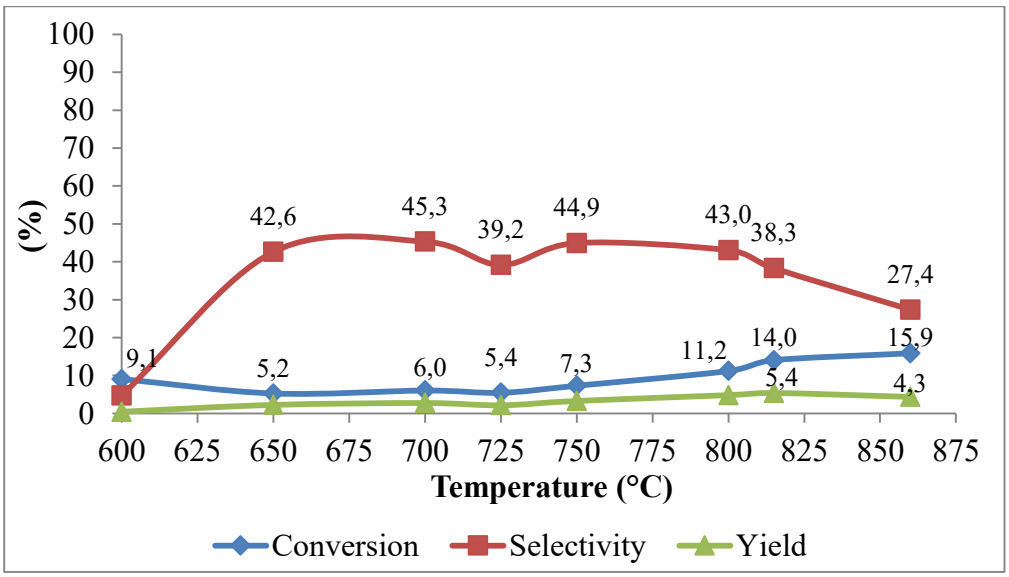

Figure 4.19. OCM performance without catalyst when CH_4/O_2=5.

Although empty reactor test demonstrated that the use of catalyst significantly improved the results over particulate catalyst and monosil, this was not the case for cordierite monolith; the selectivity and yield over this support was lower than empty reactor. Different heat transfer characteristics of the monolithic support may contributed to this result.

4.6. Heating Program for the Reactor

The way of heating the reactor to the desired temperature has important influences on the OCM reaction results; in fact variety of heating program for the reactor furnace were reported in the literature. Three different methods have been investigated in this study. Heating until the desired temperature under 10 ml.min^{-1} O_2 flow, gradual heating under 5 ml.min^{-1} N_2 flow until 400 °C, then switch to 10 ml/min O_2, heating with 10 °C/min increase and waiting 10 min at 200, 400 and 600 °C, heating until the desired temperature under 5 ml.min^{-1} N_2 flow with the same heating rate.

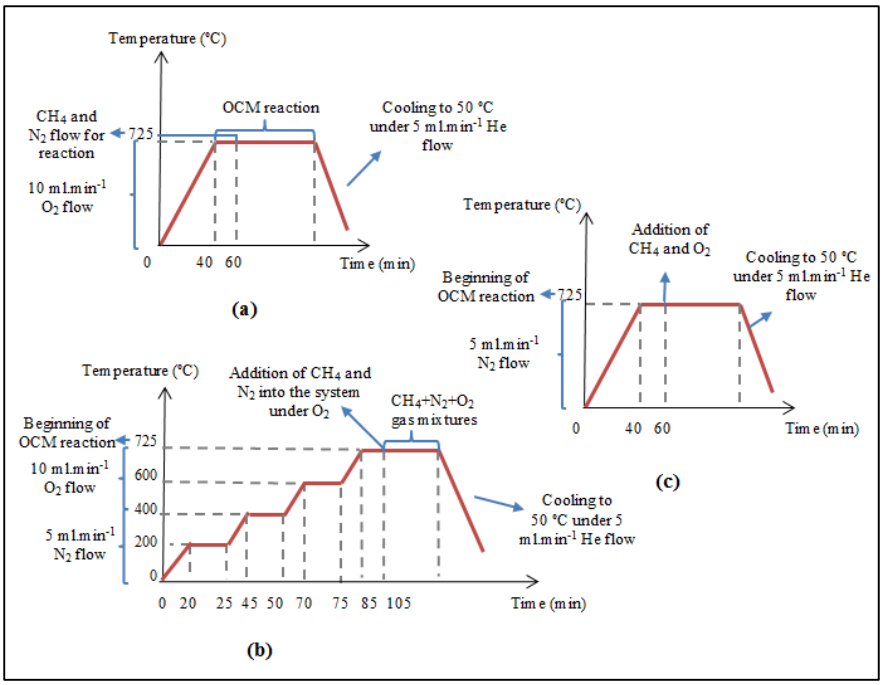

Figure 4.20. Heating of the reactor furnace; (a) heating until the desired temperature under 10 ml.min^{-1} O_2 flow, (b) heating until 400 °C under 5 ml.min^{-1} N_2 flow, then until desired temperature under 10 ml.min^{-1} O_2 flow, (c) heating under 5 ml.min^{-1} N_2 flow.

The OCM reaction was tested for each method at 725 °C and CH_4/O_2 ratio of 7 by following the procedure shown in Figure 4.20. The results have shown that the best heating mechanism was the heating under N_2 flow (c). Other two methods exhibited very close results each other.

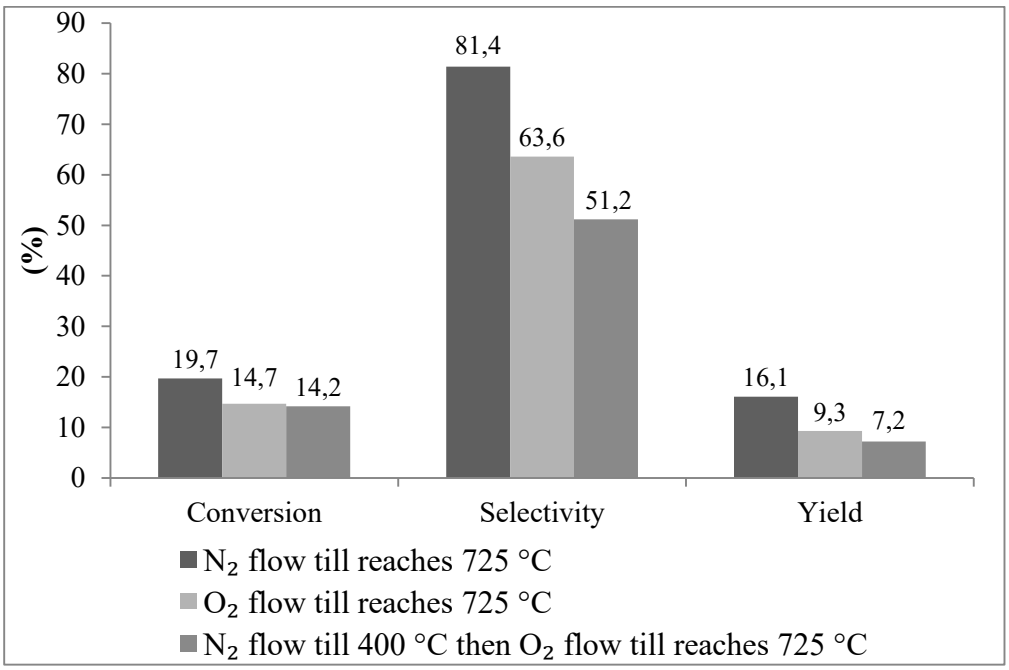

Figure 4.21. Influence of heating mechanism over OCM.

As shown in Figure 4.21 when the reactor furnace was heated under N_2 flow, C_{2+} selectivity was considerable higher than other two mechanisms. This trend was also observable for both conversion and selectivity. According to the Mleczko *et al*. (1994), high O_2 concentration causes low ethane and ethylene selectivity. When the system is heated under oxygen flow, O_2 starts to adsorb on the catalyst surface and filled the pores. After methane is fed to system, OCM reaction takes place by using atomic oxygen left during heating the reactor on the catalyst surface. Therefore, oxygen is present with a higher amount. As a result for this, non-selective gas phase reactions become dominant, subsequently a lower C_{2+} selectivity and yield is obtained. For this reason, heating with N_2 gas was chosen in this study.

5. CONCLUSION

5.1. Conclusions

2 wt.% Mn and 5 wt.% Na_2WO_4 was impregnated over supported monolithic SiO_2 in order to test the performance of oxidative coupling of methane reaction. Different types of monolithic silica were prepared and the results were compared to particulate catalyst and cordierite monolith. The major conclusions obtained from this study are listed below:

- Monosil (whole structural rod catalyst) exhibited the closest results to particulate catalyst, which can be considered as a promising preparation method for the future works.
- The highest yield, selectivity and conversion were obtained when CH_4/O_2 ratio was 5 at the temperature of 725 °C.
- The highest C_2 yield of 18.5% was obtained from the particulate catalyst prepared by incipient to wetness impregnation method, the yield of 16.0% over the monolithic silica followed that.
- Filling both the lower part of the reactor and above the catalyst bed with quartz chips ensured a high amount of desirable products by inhibiting the gas-phase reactions right after the catalyst bed.
- Since CO_x formations are thermodynamically favored in OCM, the ethane and ethylene, which are the desired products must be evacuated from the high temperature part of the reactor. For this reason, a reduced diameter of 2 mm after the catalyst bed enabled an acceleration for product gases.
- The experiments with cordierite monoliths showed that this form is not appropriate for OCM reaction due to the poor heat transfer nature of cordierite monolith. The results of cordierite monolith were even worse than reaction with blank reactor.
- The stability tests of $Mn/Na_2WO_4/SiO_2$ can be considered as a proof of the highly stable and active nature of this catalyst. After the inactive catalyst at 860 °C reduced to 750 °C, it regained its activity. This indicates that $Mn/Na_2WO_4/SiO_2$ catalyst does not need any further regeneration step to make active again.

- It was detected that the heating mechanism and the gas used during heating have crucial role to obtain best results for OCM reaction. Heating under inert N_2 gas showed the best performance.
- The CO_x formation increased when the reaction temperature enhanced. Especially, higher temperatures are favorable for CO formation. Low CH_4/O_2 ratio also caused increasing the gas-phase reaction. Therefore, methane to oxygen ratio lower than 5 was not preferred due to the high amount of the CO_x formation.

5.2. Recommendations

According to the results of this study, the following points can contribute for the future works:

- In order to prevent the deceived temperature in the catalyst bed, a second thermocouple can be inserted in the catalyst bed.
- Another support material like SiC can be used for obtaining a more stable monosils. The type of materials also provide more sufficient heat transfer and inhibit the hot spot formation since SiC is a refractory material which shows a high thermal conductivity.
- The length of the reactor can be minimized in order to prevent the gas-phase reactions.
- Another material can be added during the sol-gel preparation in order to obtain well-ordered macroporous structure. The C_{16}TAB used in this study enhanced the macropores in the structure but the strength of the monosils is low, so for more stable monosils an alternative material can be found.

REFERENCES

Alavi, S. M. and S. M. K. Shahri, 2008, "Kinetic Studies of the Oxidative Coupling of Methane over the $Mn/Na_2WO_4/SiO_2$ Catalyst", *Journal of Natural Gas Chemistry*, Vol. 18, pp. 25-34.

Alothman, Z. A., 2012, "A Review: Fundamental Aspect of Silicate Mesoporous Material", *Advances in Mesoporous Materials*, Vol. 5, No. 12, pp. 2874-2902.

Alvarez, S. and A. B. Fuertes, 2007, "Synthesis of Macro/Mesoporous Silica and Carbon Monoliths by Using a Commercial Polyurethane Foam as Sacrificial Template", *Materials Letters*, Vol. 61, pp. 2378-2381.

Amin, N. A. S. and M. K. Nikoo, 2011, "Thermodynamic Analysis of Carbon Dioxide Reforming of Methane in View of Silica Carbon Formation", *Fuel Processing Technology*, Vol. 92, pp. 678-691.

Anders, H., 2009, "Direct Conversion of Methane to Fuels and Chemicals", *Catalysis Today*, Vol. 142, No. 2, pp. 2-8.

Arndt, S., T. Otremba, U. Simon, M. Yildiz, H. Schubert and R. Schomäcker, 2012, "$Mn\text{-}Na_2WO_4/SiO_2$ as Catalyst for the Oxidative Coupling of Methane. What is really known?", *Applied General Catalysis A: General*, Vol. 425, pp. 53-61.

Babin, J., J. Iapichella, B. Lefe, C. Biolley, J. P. Bellat, F. Fajula and A. Galarneu, 2007, "MCM-41 Silica Monoliths with Independent Control of Meso- and Macroporosity", *New Journal of Chemistry*, Vol. 31, No. 11, pp. 1907-1917.

Baiker, A., R. Koirala, R. Büchel and S. E. Pratsinis, 2014, "Oxidative Coupling of Methane on Flame-made $Mn\text{-}Na_2WO_4/SiO_2$: Influence of Catalyst Composition and Reaction Conditions", *Applied Catalysis A: General*, Vol. 484, pp. 97-107.

Bialon, J. M. and A. B. Jarzebski, 2008, "Fabrication of Properties of Silica Monoliths with Ultra Large Mesopores", *Microporous and Mesoporous Materials*, Vol. 109, pp. 429-435.

Buyevskaya, O., T. D. Wolf and M. Baerns, 1994, "Surface Processes in the Catalytic Oxidative Coupling of Methane to Ethane", *Recueil des Travaux Chimiques des Pays-Bas.*, Vol. 113, pp. 459-464.

Dedov, A. G., G. D. Nipan, A. S. Loktev, A. A. Tyunyaev, V. A. Ketsko, K. V. Parkhomenko and I. I. Moiseev, 2011, "Oxidative Coupling of Methane: Influence of the Phase Composition of Silica-based Catalysts", Vol. 406, pp. 1-12.

Düşova, Y., 2014, *An Experimental Study on Oxidative Coupling of Methane over $Mn/Na_2WO_4/SiO_2$ Catalyst*, M. S. Thesis, Boğaziçi University.

Ekstrom, A., R. Regtop and S. Bhargava, 1989, "Effect of Pressure on the Oxidative Coupling Reaction of Methane", *Division of Fuel Technology*, Vol. 62, No. 1, pp. 253-269.

Farrauto, R. J., S. Gulati and M. H. Ronald, 2001, "The Application of Monoliths for Gas Phase Catalytic Reactions", *Chemical Engineering Journal*, Vol. 82, pp. 149-156.

Farsi, A., S. Ghader, A. Muradi, S. S. Mansouri and V. Shadravan, 2011, "A Simple Kinetic Model for Oxidative Coupling of Methane over $La_{0.6}Sr_{0.4}Co_{0.8}Fe_{0.2}O_{3-\delta}$ Nanocatalyst, *Journal of Natural Gas Chemistry*, Vol. 20, pp. 325-333.

Galadima, A. and O. Muraza, 2016, "Revising the Oxidative Coupling of Methane to Ethylene in the Golden Period of Shale Gas: A Review", *Journal of Industrial and Engineering Chemistry*, Vol. 37, pp. 1-13.

Galarneau, A. and A. Sachse, 2010, “Synthesis of Zeolite Monoliths for Flow Continuous Processes. The Case of Sodalite as a Basic Catalyst”, *Chemistry of Materials Communication*, Vol. 22, pp. 4123-4125.,

Galarneau, A., A. Sachse, F. Fajula, F. Di Renzo, P. Creux and B. Coq, 2011, “Functional Silica Monoliths with Hierarchical Uniform Porosity as Continuous Flow Catalytic Reactors”, *Microporous and Mesoporous Materials*, Vol. 140, pp. 58-68.

Godini, H. R., A. Gili, O. Görke, S.Arndt, U. Simon, A. Thomas, R. Schomäcker and G. Wozny, 2014, “Sol-gel Method for Synthesis of Mn-Na_2WO_4/SiO_2 Catalyst for Methane Oxidative Coupling”, *Catalysis Today*, Vol. 236, Part A, pp. 12-22.

Hagelin-Weaver, H. E. and T. W. Elkins, 2015, “Characterization of Mn-Na_2WO_4/SiO_2 and Mn-Na_2WO_4/MgO Catalysts for the Oxidative Coupling of Methane”, *Applied Catalysis A: General*, Vol. 497, pp. 96-106.

Huerta, L., C. Guillem, J. Latorre, A. Beltran, D. Beltran and P. Amoros, 2005, “Silica-based Macrocellular Foam Monoliths with Hierarchical Trimodal Pore Systems”, *Solid State Sciences*, Vol.7, pp.405-414.

Iglesia, E. and K. Takanabe, 2009, “Mechanistic Aspects and Reaction Pathways for Oxidative Coupling of Methane on Mn/Na_2WO_4/SiO_2 Catalysts”, *The Journal of Physical Chemistry*, Vol. 23 No. 113, pp. 10131-10145.

Ito, T., J. Wang, C. H. Lin and J. H. Lunsford, 1985, “Oxidative Dimerization of Methane over a Lithium-promoted Magnesium-oxide Catalyst”, *American Chemical Society*, Vol. 107, No. 18, pp. 5062-5068.

Ji, S., T. Xiao, S. Li, L. Chou, B. Zang, C. Xu, R. Hou, A. P. E. York and M. L. H. Green, 2003, “Surface WO_4 Tetrahedron: the Essence of the Oxidative Coupling of Methane over M-W-Mn/SiO_2 Catalysts”, *Journal of Catalysis*, Vol. 220, No. 1, pp. 47-56.

Jiang, Z. C., C. J. Yu, X. P. Fang, S. B. Li and H. L. Wang, 1993, "Oxidative/Support Interaction and Surface Reconstruction in the Sodium Tungstate (Na_2WO_4)/Silica System", *The Journal of Physical Chemistry*, Vol. 97, No. 49, pp. 12870-12875.

Khimich, N. N., 2004, "On the Problem of Drying of a Monolithic Silica Gel", *Glass Physics and Chemistry*, Vol. 30, No. 1, pp.107-108.

Kirschning, A., C. Altwicker, G. Drager, J. Harders, N. Hoffmann, U. Hoffmann, H. Schönfeld, W. Solodenko and U. Kunz, 2001, "Pass Flow Syntheses Using Functionalized Monolithic Polymer/Glass Composites in Flow-Through Microreactors"*, Angewandte Chemie International Edition*, Vol. 40, pp. 3995-3998.

Kondratenko, E. and M. Baerns, 2008, *Handbook of Heterogeneous Catalysis*, Wiley, Weinheim.

Kooh, A., J. L. Dubois, H. Mimoun and C. J. Cameron, 1990, "Oxidative Coupling of Methane: Maximizing the Yield of Coupling Products under Cofeed Operating Conditions", *Catalysis Today*, Vol. 6, pp. 453-462.

Korf, S. J., J. A. Roos, L. J. Veltman, J. G. Van Ommen and J. R. H. Ross, 1989, "Effect of Additives on Lithium Doped Magnesium Oxide Catalysts Used in the Oxidative Coupling of Methane", *Applied Catalysis*, Vol. 56, pp. 119-135.

Kunz, U., A. Kirschning, H. L. Wen, W. Solodenko, R. Cecilia, C. O. Kappe and T. Turek, 2005, "Monolithic Polymer/Carrier Materials: Versatile Composites for Fine Chemical Synthesis", *Catalysis Today*, Vol. 105, pp. 318-324.

Li, S., J. Wang, L. Chou, B. Zhang, H. Song, J. Zhao and J. Yang, 2006, "Comparative Study on Oxidation of Methane to Ethane and Ethylene Over Na_2WO_4-Mn/SiO_2 Catalysts Prepared by Different Methods", *Journal of Molecular Catalysis A: Chemical*, Vol. 245, pp. 272-277.

Lunsford, J. H., 2000, "Catalytic Conversion of Methane to More Useful Chemicals and Fuels: A Challenge for the 21st Century", *Catalysis Today*, Vol. 63, No. 2-4, pp. 165-174.

Lunsford, J. H., 1995, "The Catalytic Oxidative Coupling of Methane", *Angewandte Chemie International Edition in English*, Vol. 34, No. 9, pp. 970-980.

Machado, M., R. R. Broekhuis, A. F. Nordquist, P. R. Brian and R. Steven, 2005, "Applying Monolith Reactors for Hydrogenations in the Production of Specialty Chemicals-Process and Economic Considerations", *Catalysis Today*, Vol. 105, pp. 305-317.

Martin, J., B. Hosticka, C. Lattimer and P. M. Norris, 2011, "Mechanical and Acoustical Properties as a Function of PEG Concentration in Macroporous Silica Gels", *Journal of Non-Crystalline Solid*, Vol. 285, pp. 222-229.

Malekzadeh, A., A. A. Khodadadi, M. Amini, H. K. Mishra and A. K. Dalai, 2002, "Oxidative Coupling of Methane over Oxide-Supported Sodium-Manganese Catalyst", *Catalysis Letters*, Vol. 84, pp. 45-51.

McQuade, B. P., K. E. Price, J. L. Steinbacher, A. R. Bogdan and B. P. Mason, 2007, "Greener Approaches to Organic Synthesis Using Microreactor Technology", *Chemical Reviews*, Vol. 107, No. 6, pp. 2300-2318.

Mesa, M., L. Sierra, L. F. Giraldo, B. L. Lopez, L. Perez and S. Urrego, 2007, "Mesoporous Silica Applications", *Macromolecular Symposia*, Vol. 258, No. 1, pp. 129-141.

Mleczko, L., D. Schweer, Z. Durjanova, R. Andorf and M. Baerns, 1994, "Reaction Engineering Approaches to the Oxidative Coupling of Methane to C_{2+} Hydrocarbons", *Natural Gas Conversion II*, Vol. 81, pp. 155-164.

Mleczko, L. and M. Baerns, 1995, "Catalytic Oxidative Coupling of Methane-Reaction Engineering Aspects and Process Schemes", *Fuel Processing Technology*, Vol. 42, pp. 217-248.

Mleczko, L., Z. Stansch and M. Baerns, 1997, "Comprehensive Kinetics of Oxidative Coupling of Methane over the La_2O_3/CaO Catalyst", *Industrial & Engineering Chemistry Research*, Vol. 36, pp. 2568-2579.

Moulijn, J. A., T. A. Nijhuis, J. J. Heiszwolf and F. Kapteijn, 2001, "New Non-traditional Multiphase Catalytic Reactors Based on Monolithic Structures", *Catalysis Today*, Vol. 66, pp. 133-144.

Nadjafi, M., 2015, *Oxidative Coupling of Methane over Lithium Doped Magnesium Oxide*, M. S. Thesis, Boğaziçi University.

Nakanishi, K. and N. Soga, 1992, "Phase Separation in Silica Sol-gel System Containing Polyacrylic Acid. I. Gel Formation Behavior and Effect of Solvent Composition", *Journal of Non-crystalline Solids*, Vol. 139, pp. 1-13.

Nishihara, H., S. R. Mukai, Y. Fujii, T. Tago, T. Masuda and H. Tamon, 2006, "Preparation Monolithic Silica SiO_2-Al_2O_3 Cryogels with Inter-connected Macropores through Ice Templating", *Journal of Materials Chemistry*, Vol. 16, pp. 3231-3236.

Thien, C.Y., M. A. Rahman and B. Subhash, 2008, "Oxidative Coupling of Methane for the Production of Ethylene over Sodium-Tungsten-Manganese-Supported Silica Catalyst (Na-W-Mn/SiO_2)", *Applied Catalysis A: General*, Vol. 343, No. 4, pp. 142-148.

Palermo, A., J. P. Vazquez, A. F. Lee, S. Mintcho, R. M. Lambertz and T. Lambert, 1998, "Critical Influence of the Amorphous Silica-to-Cristobalite Phase Transition on the Performance of Mn/Na_2WO_4/SiO_2 Catalysts for the Oxidative Coupling of Methane", *Journal of Catalysis*, Vol. 177, pp. 259-266.

Oye, G., B. Gawel and K. Gawel, 2010, "Sol-gel Synthesis of Non-silica Monolithic Materials", *Materials*, Vol. 3, pp. 2815-2833.

Rane, V. H., S. T. Chaudhari and V. R. Choudhary, 2008, "Influence of Alkali Metal Doping on Surface Properties and Catalytic Activity/Selectivity of CaO Catalysts in Oxidative Coupling of Methane", *Journal of Natural Gas Chemistry*, Vol. 17, No.4, pp. 313-320.

Rodemerck, U., P. Ignaszweski, M. Lucas and P. Claus, 2000, "Parallel Synthesis and Fast Catalytic Testing of Catalyst Libraries for Oxidation Reactions", *Chemical Engineering and Technology*, Vol. 23, No. 5, pp. 413-416.

Sachse, A., V. Hulea, A. Finiels, B. Coq, F. Fajula and A. Galarneau, 2012, "Alumina-grafted Macro-/Mesoporous Silica Monoliths as Continuous Flow Microreactors for The Diels-Alder Reaction", *Journal of Catalysis*, Vol. 287, pp. 62-67.

Sachse, A., A. El Kadib, R. Chimenton, F. Fajula, A. Galarneau and B. Coq, 2009, "Functionalized Inorganic Monolithic Microreactors for High Productivity in Fine Chemicals Catalytic Synthesis", *Journal of Catalysis,* Vol. 48, pp. 4969-4972.

Salehoun, V., A. Khodadadi, Y. Mortazavi and A. Talebizadeh, 2008, "Dynamic of $Mn/Na_2WO_4/SiO_2$ Catalyst in Oxidative Coupling of Methane", *Chemical Engineering Science*, Vol. 63, No. 20, pp. 4910-4916.

Schomäcker, R., B. Beck, V. Fleischer, S. Arndt, M.G. Hevia, A. Urakawa and P. Hugo, 2013, "Oxidative Coupling of Methane-A Complex Surface/Gas Phase Mechanism with Strong Impact on the Reaction Engineering", *Catalysis Today,* Vol. 228, pp. 212-218.

Schuurman, Y., T. Serres, C. Aquino and C. Mirodatos, 2014, "Influence of the Composition/Texture of Mn-Na-W Catalysts on the Oxidative Coupling of Methane", *Applied Catalysis A:* General, Vol. 504, pp. 509-518.

Sergei, P. and Lunsford J. H., 1998, "Thermal Effects during the Oxidative Coupling of Methane over $Mn/Na_2WO_4/SiO_2$ and $Mn/Na_2WO_4/MgO$ Catalysts", *Applied Catalysis A: General*, Vol. 168, No. 1, pp. 131-137.

Shahri, S. M. and A. N. Pour, 2009, "Ce-promoted $Mn/Na_2WO_4/SiO_2$ Catalyst for Oxidative Coupling of Methane at Atmospheric Pressure", *Journal of Natural Gas Chemistry,* Vol. 19, pp. 47-53.

Sheng-Fu, J., S. B. Li, Y. Liu, L. Gao, J. Z. Niu and C. Z. Xu, 1999, "Role of Sodium in the Oxidative Coupling of Methane", *Chemical Engineering Science*, Vol. 8, No. 1., pp. 1182-1192.

Shi, Z. G., Y. Q. Feng, L. Xu and S. L. Da, 2003, "Preparation of Porous Carbon-Silica Composite Monoliths", *Letters to the Editor/Carbon*, Vol. 41, pp. 2653-2689.

Siouffi, A. M., 2003, "Silica Gel-based Monoliths Prepared by the Sol-gel Method: Facts and Figures", *Journal of Chromatography: A*, Vol. 1000, pp. 801-818.

Smatt, J. Hi Schunk S. and M. Linden, 2003, "Versatile Double-templating Synthesis Route to Silica Monoliths Exhibiting a Multimodal Hierarchical Porosity", *American Chemical Society*, Vol. 15, No. 12, pp. 2354-2361.

Sofranko, J. A., J. J. Leonard and C. A. Andrew, 1986, "The Oxidative Conversion of Methane to Higher Hydrocarbon", *Journal of Catalysis*, Vol. 103, pp. 302-310.

Somayeh, M. and M. Reza, 2011, "Effect of Additives on Mn/SiO_2 Based Catalyst on Oxidative Coupling of Methane", *Iranian Journal of Chemistry Engineering*, Vol. 30, No. 1. pp. 29-36.

Suh, D. J., J. M. Ha, J. Y. Lee, W. Jeon, J. W. Choi and Y. W. Suh, 2013, "Scaled-up Production of C_2 Hydrocarbons by the Oxidative Coupling of Methane over

Pelletized Na_2WO_4/SiO_2 Catalysts: Observing Hot Spots for the Selective Process", *Fuel*, Vol. 106, pp. 851-857.

Tomastic, V. and F. Jovic, 2006, "State-of-the-art in the Monolithic Catalysts/Reactors", *Applied Catalysis A: General*, Vol. 311, pp. 112-121.

Watts, P. and C. Wiles, 2006, "Recent Advances in Synthetic Micro Reaction Technology", *The Royal Society of Chemistry*, Vol. 5, pp. 443-467.

Williams, J. L., 2001, "Monolith Structures, Materials, Properties and Uses", *Catalysis Today*, Vol. 69, pp. 3-9.

Wirth, T., B. Ahmed-Omer and J. C. Brandt, 2006, "Advanced Organic Synthesis Using Microreactor Technology", *Organic & Biomolecular Chemistry.*, Vol. 5, No. 5, pp. 733-740.

Witoon, T. and M. Chareonpanich, 2012, "Synthesis of Hierarchical Meso-Macroporous Silica Monolith Using Chitosan as Biotemplate and Its Application as Polyethyeneimine Support for CO_2 Capture", *Materials Letters*, Vol. 81, pp. 181-184.

Wu, J. and S. Li, 1995, "The Role of Distorted WO_4 in the Oxidative Coupling of Methane on Tungsten Oxide", *The Journal of Physical Chemistry*, Vol.99, pp. 4566-4568.

Thirugnanam, T., 2013, "Effects of Polymers (PEG and PVP) on Sol-gel Synthesis of Microsized Zinc Oxide", *Journal of Nanomaterials*, Vol. 2013.

Zavyalova, U., M. Holena and R. Schlögl, 2011, "Statistical Analysis of Past Catalytic Data on Oxidative Methane Coupling for New Insights into the Composition of High-performance Catalysts", *Chemcatchem*, Vol. 3, No. 12, pp. 1935-1947.